NASA TECHNICAL NOTE

NASA TN D-4500

INVESTIGATION OF TEMPERATURE MEASUREMENTS IN 300° TO 1100° K LOW-DENSITY AIR USING AN ELECTRON BEAM PROBE

by William W. Hunter, Jr.

Langley Research Center
Langley Station, Hampton, Va.

NATIONAL AERONAUTICS AND SPACE ADMINISTRATION • WASHINGTON, D. C. • MAY 1968

INVESTIGATION OF TEMPERATURE MEASUREMENTS IN 300° to 1100° K LOW-DENSITY AIR USING AN ELECTRON BEAM PROBE

By William W. Hunter, Jr.

Langley Research Center
Langley Station, Hampton, Va.

NATIONAL AERONAUTICS AND SPACE ADMINISTRATION

For sale by the Clearinghouse for Federal Scientific and Technical Information
Springfield, Virginia 22151 – CFSTI price $3.00

INVESTIGATION OF TEMPERATURE MEASUREMENTS IN 300° to 1100° K LOW-DENSITY AIR USING AN ELECTRON BEAM PROBE*

By William W. Hunter, Jr.
Langley Research Center

SUMMARY

Laboratory measurements of rotational and vibrational temperatures have been performed over a range from 300° to 1100° K in static low-density air with an electron beam probe. The tests were conducted in a unique test chamber which permitted the selection of various combinations of test pressures and temperatures.

Rotational-temperature measurements were made from the (0,0) band of the first negative system of the nitrogen constituent of air. Some tests were also performed by using the (0,1) band of the first negative system of nitrogen. No substantial differences were noted between the results of the (0,1) band tests and those of the (0,0) band tests.

The accuracy of the measured rotational temperatures was found to vary with gas temperature and gas number density. A difference existed between the measured rotational temperature and the gas temperature. This difference increased with increasing gas temperature. With the inclusion of an experimentally determined correction for the gas-number-density effect, the rotational-temperature measurements were made with an accuracy that varied from approximately 0 to -6 percent with increasing gas temperature.

Vibrational-temperature measurements were made by using the intensity ratios of the (0,1) and (1,2) bands of the first negative system of nitrogen. The measurements were found to be within ±20 percent of the gas temperature.

INTRODUCTION

The present investigation was undertaken as part of a continuing instrument development program of the Langley Research Center. This particular effort was directed

*Part of the material presented in this report is included in a thesis entitled "Measurement of $N_2X^1\Sigma_g^+$ Rotational and Vibrational Temperatures Over a 300° K to 1100° K Range Using a High-Energy Electron Beam" submitted in partial fulfillment of the requirements for the degree of Master of Arts in Physics, The College of William and Mary in Virginia, August 1965.

towards the verification of a technique for measuring free-stream temperatures of low-density hypersonic wind tunnels which use air or nitrogen.

The technique consists of passing a beam of high-energy (10- to 30-kV) electrons through a low-density gas. The electrons have inelastic collisions with gas molecules and these excited ionized molecules provide fluorescence. A spectral analysis of the fluorescence provides a means for determining molecular gas rotational and vibrational temperatures.

The initial investigator, E. P. Muntz (ref. 1), experimentally verified his theoretical model for the electron beam probe technique for two temperatures, $\approx 300^{\circ}$ K and 373° K. These experiments were conducted in a low-velocity (0.5-m/sec) flow of nitrogen gas, and the data were obtained from the (0,0) band of the first negative system of nitrogen. Since the original work, others (refs. 2, 3, 4, and 5) have used the technique for diagnostic wind-tunnel measurements. In reference 4, the calculated tunnel parameters are compared with the measured rotational temperatures as a test of the theory for temperatures below 300° K.

The purpose of the present work was to verify experimentally the theory for rotational- and vibrational-temperature measurements for a range of temperatures from 300° to 1100° K under controlled conditions in the laboratory. These tests were conducted in a static test gas, air. The rotational-temperature measurements were made from data obtained from the (0,0) band of nitrogen. Rotational-temperature measurements were also made from data obtained from the (0,1) band of the first negative system of nitrogen for comparison with results obtained from the (0,0) band. The vibrational-temperature measurements were made from data obtained from the (0,1) and (1,2) bands. Tests were conducted in nitrogen as well as in air to determine whether there were any significant differences in the resulting temperature measurements.

SYMBOLS

(A)	term defined by equation (25)
$A_{K'K_2''}$	transition probability for emission between rotational energy states K' and K_2'' (see eq. (23))
A_{nm}	transition probability for emission between states n and m
$A_{v'v_2''}$	transition probability for emission between vibrational energy states v' and v_2''

B_0	rotational constant related to vibrational level $v_1'' = 0$
$B^2\Sigma_u^+$	electronic wave function for $N_2^+B^2\Sigma_u^+$
C_e	excitation function which described electron-molecular excitation process
$\hat{C}_e$	ratio of excitation function to depopulation rate of $N_2^+B^2\Sigma_u^+$ state
c	speed of light
$E_{K_1''}$	characteristic energy of rotational energy level K_1''
$E_{v_1''}$	characteristic energy of vibrational energy level v_1''
e	electron charge
e_p	initial wave function of primary electron
$\hat{e}_p$	final wave function of primary electron
e_s	wave function of secondary electron
$F(K_1'')$	rotational term (ref. 9)
$[G]$	defined by equation (30)
$G_o(v_1'')$	vibrational term (ref. 9)
h	Planck's constant
$I_{K'K_2''}$	intensity of emission for transitions between K' and K_2'' rotational energy levels
I_{nm}	intensity of emission for transitions between n and m states
I_o	reference intensity of emission
$I_{v'v_2''}$	intensity of emission for transitions between v' and v_2'' vibrational energy levels

J	quantum number of total angular momentum
K	rotational quantum number
ΔK	change of rotational quantum number
k	Boltzmann's constant
M	quantum number of a component of total angular momentum
N_K	steady-state number density population of a rotational energy level
N_n	number density population of state n
N_o	steady-state number density population of $N_2 X^1\Sigma_g^+$
N_v	steady-state number density population of a vibrational energy level
N_2	neutral nitrogen
N_2^+	ionized nitrogen
$N_2^+ B^2\Sigma_u^+$	excited ion state of N_2^+
$N_2 X^1\Sigma_g^+$	ground state of N_2
$N_2^+ X^2\Sigma_g^+$	ground state of N_2^+
n	gas number density
n_o	reference gas number density, 3×10^{-14} cm^{-3}
P_R^a	relative rotational line strength for excitation
P_{RR}^a, P_{RP}^a	relative rotational line strength for excitation for R branch and P branch, respectively
P_R^e	relative rotational line strength for emission

$P_{v'v''}$	band strength
Q_r	rotational partition function
Q_v	vibrational partition function
$q_{v'v''}$	Franck-Condon factor
$\bar{q}$	momentum transfer term
R	depopulation rate of $N_2^+B^2\Sigma_u^+$
R_{ij}	electronic transition moment for electronic states i and j
r_n	nuclei separation
r_{1i}	distance between primary and ith orbital electrons
r_{12}	distance between primary and secondary electrons
$\bar{r}_i$	position vector of ith orbital electron
$\bar{r}_1$	position vector of primary electron with respect to point of observation
$\bar{r}_2$	position vector of secondary electron with respect to point of observation
$\bar{r}_2^*$	position vector of secondary electron with respect to molecular axis
$S_{K''}^{K'}$	Hönl-London factor (ref. 9)
T	gas temperature
T_r	rotational temperature
T_v	vibrational temperature
v	vibrational energy state
W	constant defined in equation (26)

X	constant in equation (23)
$X^1\Sigma_g^+$	electronic wave function for $N_2X^1\Sigma_g^+$
Y	constant defined in equation (29)
Z	constant in equations (1) and (31)
θ,χ,ϕ	Euler angles
Λ	quantum number of resultant electronic orbital angular momentum
ν	wave number
ν_o	reference wave number
ν_{nm}	wave number of (n,m) transition
$\nu_{v'v''_2}$	wave number of $\left(v_1,v''_2\right)$ transition
$\sigma_u 2s$	angular characteristics of an orbital electron of $N_2X^1\Sigma_g^+$ (ref. 9)
ψ_e	electronic-state wave function
$\psi_{evJ\Lambda M}$	molecular wave function
$\psi_{J\Lambda M}$	rotational-state wave function
ψ_v	vibrational-state wave function

Superscripts:

'	excited ionized state of nitrogen, $N_2B^2\Sigma_u^+$
''	ground state of neutral nitrogen or ionized nitrogen

Subscripts:

a	vibrational energy state a of excited ionized nitrogen
b	vibrational energy state b of excited ionized nitrogen

1 ground state of neutral nitrogen, $N_2X^1\Sigma_g^+$

2 ground state of ionized nitrogen, $N_2X^2\Sigma_g^+$

EXPERIMENTAL SYSTEM

Test Chamber and Control System

The test chamber and control system, shown in figure 1, was designed to provide flexibility in temperature and vacuum test conditions. Temperature and pressure operating ranges are approximately 300^o to 1100^o K and 6.7 to 133.3×10^{-3} N/m^2.

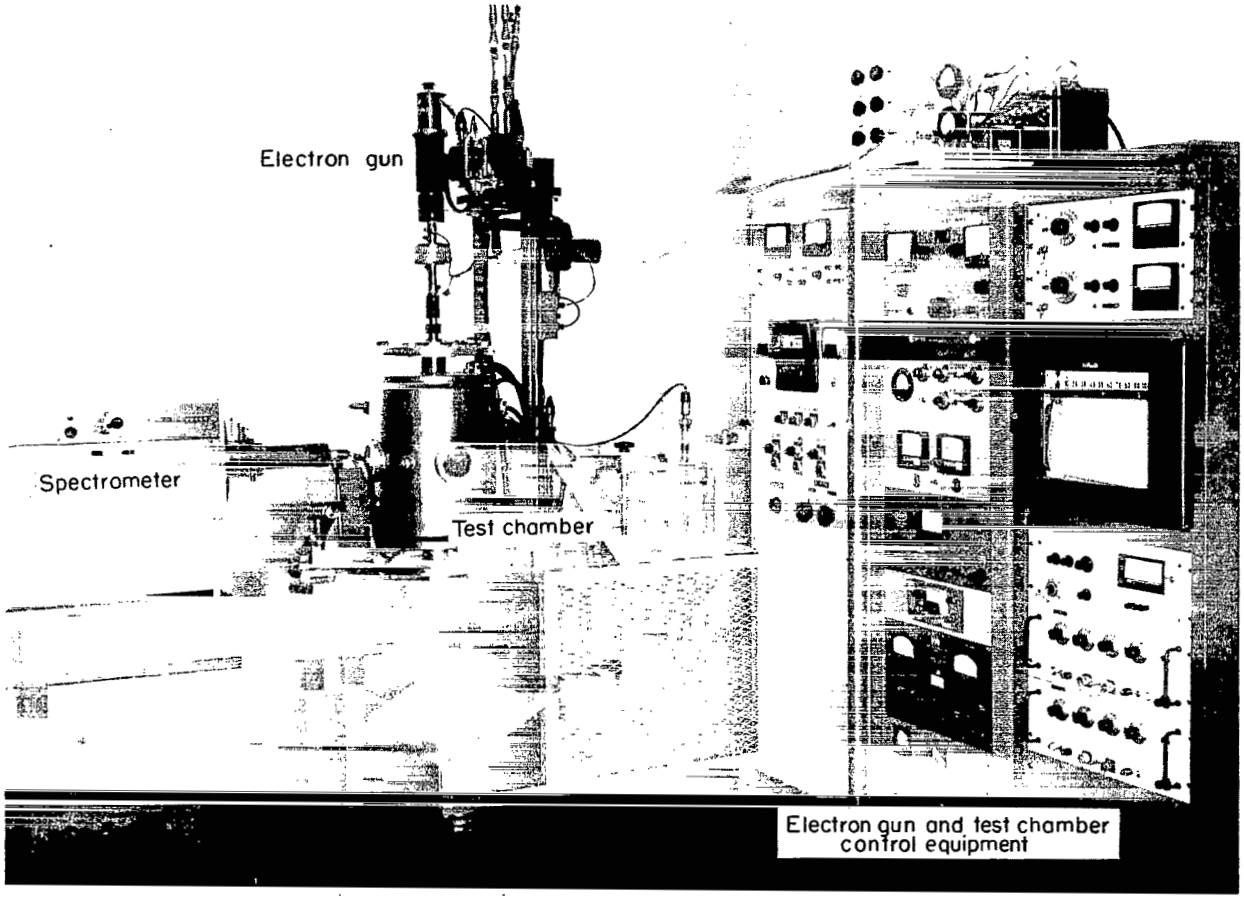

Figure 1.- Experimental apparatus. L-66-7099.1

The major component of the system is the test chamber (fig. 2), which consists of three concentric cylinders. The outer cylinder is a stainless-steel water-cooled jacket and is fitted with vacuum-tight water-cooled top and bottom covers. Each cover is fitted with large flanges, attached to extensions, for mounting test hardware. Three 7.6-cm-diameter optical-grade-quartz windows are located in the outer cylinder wall. The next concentric cylinder consists of a helically wound nickel-ribbon heating element and is attached to ceramic supporting rods. Electrical connections are made to copper electrodes which extend through the outer cylinder. The inner cylinder is a 20-cm-diameter, 38-cm-long stainless-steel electrostatic shield and is grounded together with

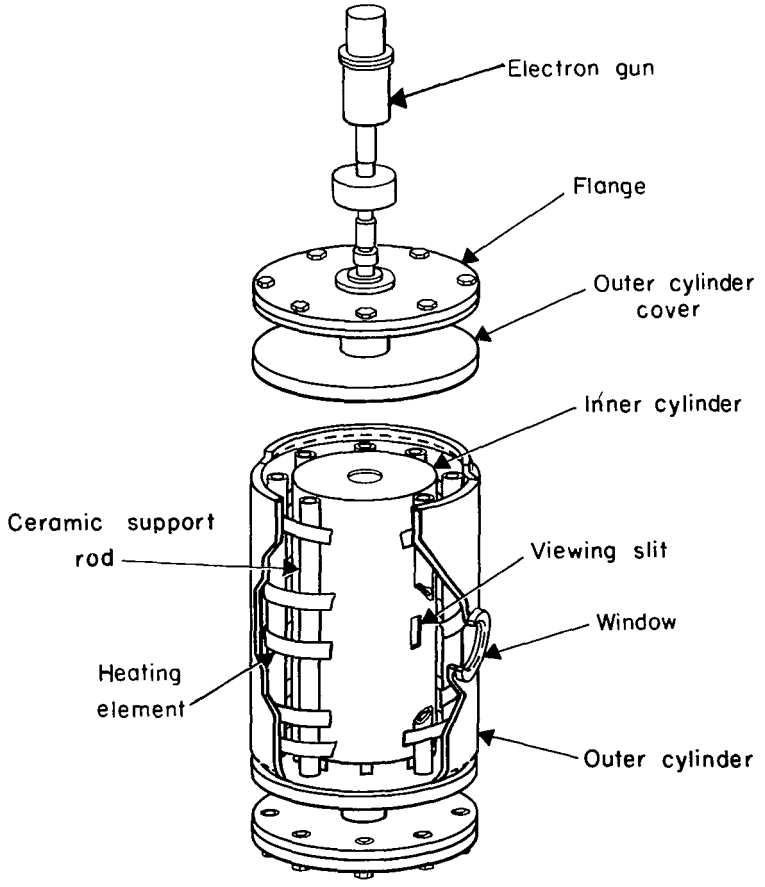

Figure 2.- Test chamber and electron gun.

the outer cylinder to prevent charge buildup on the walls. Also, the inner cylinder provides a more uniform heating surface for the test gas than would be provided by the ribbon heating element. The inner cylinder is equipped with end covers which have openings for passage of the electron beam. A 3.8- by 1.3-cm slit opening is provided in the cylinder wall and is located in line with one of the viewing windows of the outer cylinder.

Rectified heater current is supplied from a 440-V ac three-phase system. Temperature control is provided by coarse and fine rheostats. Temperature is regulated within ±1 percent of the preset value by an on-off automatic pyrometer. An operating temperature of 1100° K is obtained for a heating-element voltage of 35 V dc and a current of 50 amperes.

A 35-psi (241-kN/m^2) water-cooling system provides a heat sink for the outer chamber wall and covers and cools the diffusion pump. An interlock system prevents operation of the heating system and diffusion pump unless proper cooling flow is established.

A 5-ft^3/min (0.002-m^3/sec) mechanical pump, 750-liter/sec (0.75-m^3/sec) diffusion pump, cold trap, and necessary isolating valves comprise the vacuum pumping system. A variable leak valve with air dryer, in combination with the mechanical pump, was used to maintain the test chamber at the desired pressure. For all experiments, the chamber pressure was measured with a McLeod gage.

Test-Chamber Temperature Survey

A series of tests was conducted to establish the test-chamber gas temperature. First, a survey of the inner-cylinder wall was made to determine the temperature variation of the heating surface. This survey was performed with 12 thermocouples attached to the inner-cylinder wall and located to give reasonable coverage. The results indicated that a ±20° variation existed at 1100° K. This variation decreased with decreasing temperature.

The inner-cylinder ends were not in close proximity to the heating element and were, therefore, cooler than the side walls. The second test was made to determine the effects of these cooler surfaces on the test gas at the point of observation. A thermocouple was located on the bottom end plate near the chamber center line. The temperature of this point was the lowest temperature of the plate. The temperature along the center line was calculated from a solution of Laplace's equation in cylindrical coordinates. It was assumed in this solution that the temperature varied linearly along the length of the cylinder and was constant about the circumference. This assumption was justified on the basis of the data obtained from the tests described in the preceding paragraph.

The results of the calculations show that the effects of the inner-cylinder ends would lower the gas temperature at the midpoint of the cylinder no more than 4^{o} at 1100^{o} K.

The final test was a direct measurement of the test gas translational temperature (hereafter referred to as gas temperature) at the point of observation. These measurements were made with a thermocouple whose leads were brought in along the chamber center line and the junction located at the point of observation. Two thermocouple sizes, 0.1-mm and 0.5-mm diameter, were used to determine whether there were significant heat losses due to thermocouple conduction at the point of observation. The data show that conduction losses were negligible. The results are indicated in figure 3, which is a plot of the difference between the gas temperature, measured with the thermocouples, and the reference wall temperature as a function of the test-chamber inner-cylinder reference wall temperature. These data show that the gas temperature at the point of observation is lower than the reference wall temperature. This difference decreases with a decrease in temperature and is attributed to heat sinks provided by the observation and pumping ports.

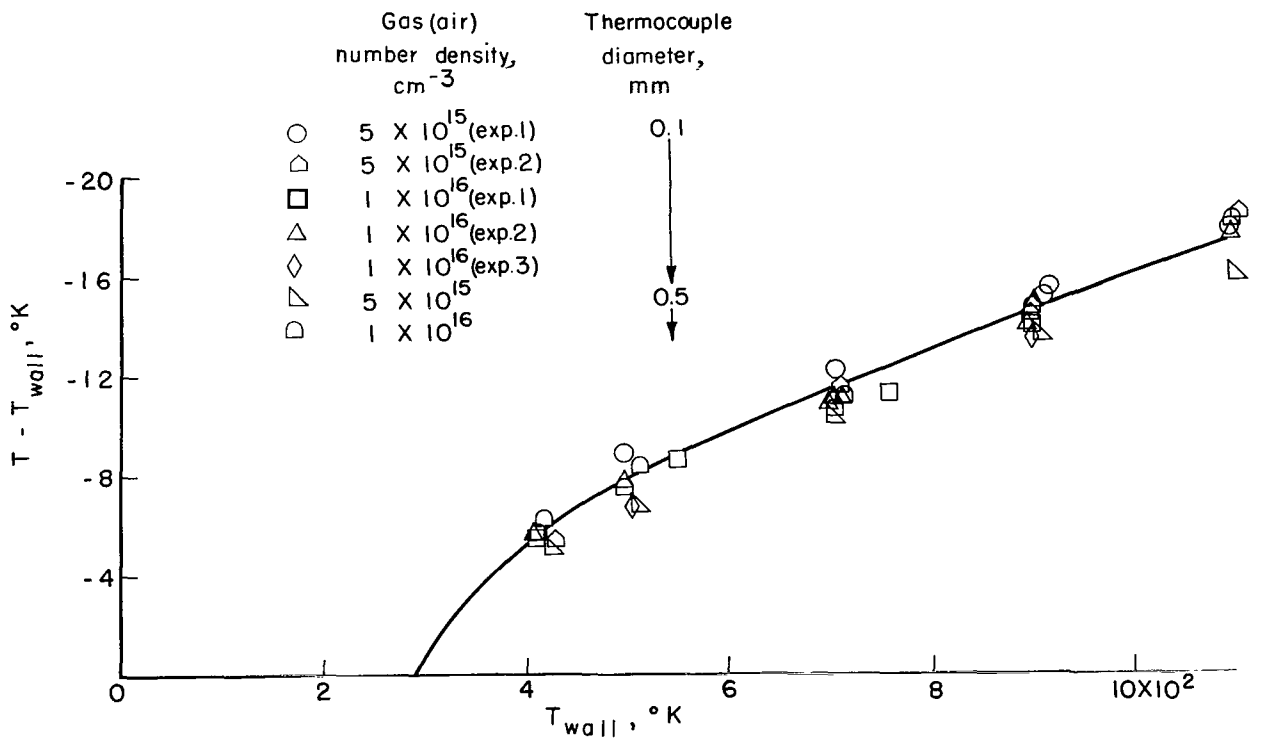

Figure 3.- Test-chamber wall temperature as a function of difference between wall temperature and gas temperature.

Electron Beam System

The electron gun (fig. 4) is a conventional point cathode system which has a directly heated hairpin tungsten filament, independent negative grid bias for current control, and cathode focusing. The beam is magnetically focused and deflected upon passage into the

drift tube. The focused beam passes through a 1.0-mm-diameter hole in a 2.5-cm-long plug which is placed in the end of the drift tube. Because of the low gas conductance of this passage through the plug, the test chamber may be operated at pressures up to 133 N/m^2 while the gun is maintained within acceptable pressure range, ≤ 2.7 cN/m^2.

The beam system was operated at potentials between 25 and 30 kV and currents between 1.0 to 1.5 mA. The beam potential and currents were held constant within ± 1 percent of the selected values for all tests.

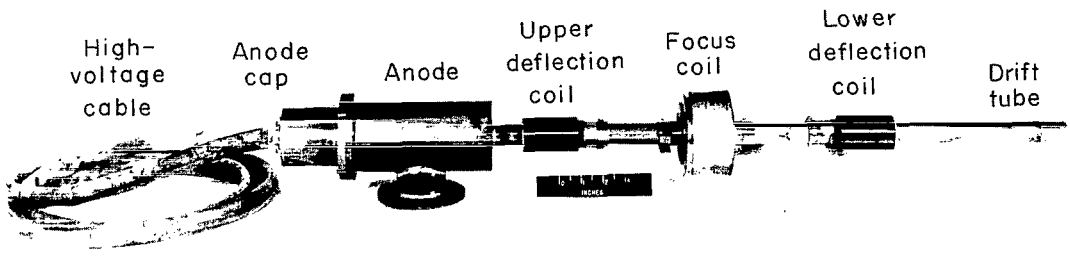

Figure 4.- Electron gun and anode assembly. L-68-810

Optical and Electronic Detector System

The major component of the optical and electronic detector system is the 0.5-meter scanning spectrometer. This instrument has 16.0-Å/mm dispersion in the first order and 0.2-Å resolution. A 13-stage venetian-blind photomultiplier tube which has an S-13 spectral response characteristic is mounted at the exit slit. The photomultiplier output is fed into an electrometer amplifier which drives a strip-chart recorder. The overall response of the system is approximately 1 second. Because the response of the available system was relatively slow, a 5-Å/min scanning speed was used.

ROTATIONAL-TEMPERATURE MEASUREMENTS

Tests

Rotational-temperature measurements were made in air from the (0,0) band of the first negative system of nitrogen at approximately 100° intervals from 300° to 1000° K. Two sets of tests were performed with a constant gas number density of 1×10^{16} cm^{-3} and the other set, with a constant gas number density of 5×10^{15} cm^{-3}. Typical spectral traces are shown in figure 5. For all rotational-temperature tests, the width of the spectrometer entrance slits were selected so that the intensity of each line could be determined from the peak value of each line.

The procedure for obtaining the rotational-temperature measurement was to determine the relative peak value of a rotation spectral line and to enter this value for $I_{K'K''_2}$

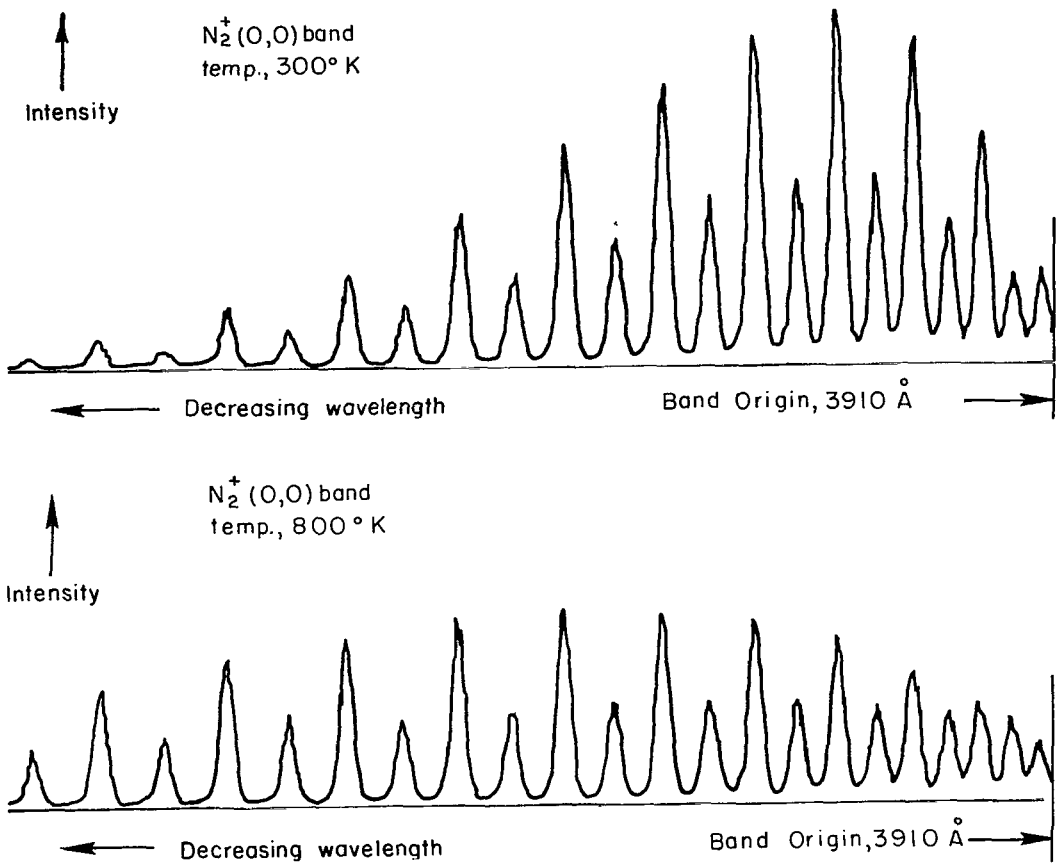

Figure 5.- Typical spectra of N_2^+ (0,0) band. R branch.

into the following equation, which is derived in the appendix:

$$\frac{B_0 hc}{kT_r} K'(K' + 1) + Z = -2.3 \log_{10} \frac{I_{K'K_2''}/I_o}{\left(K' + K_2'' + 1\right)\left[[G]\left(\nu/\nu_o\right)^4\right]} \tag{1}$$

A plot of the value of $-2.3 \log_{10} \frac{I_{K'K_2''}/I_o}{\left(K' + K_2'' + 1\right)\left[[G]\left(\nu/\nu_o\right)^4\right]}$ against $K'(K' + 1)$ provides a datum point for each spectral line. The two curves in figures 6 and 7 are obtained by a least-squares fit to the data points. One curve represents the odd K' lines (strong line system) and the second curve represents the even K' lines (weak line system). The slopes of the curves are equal to $\frac{B_0 hc}{kT_r}$, and from this equality the rotational temperature T_r is determined. The final value of the rotational temperature is determined from a weighted mean of the values obtained from the two curves. The weighting is in accordance

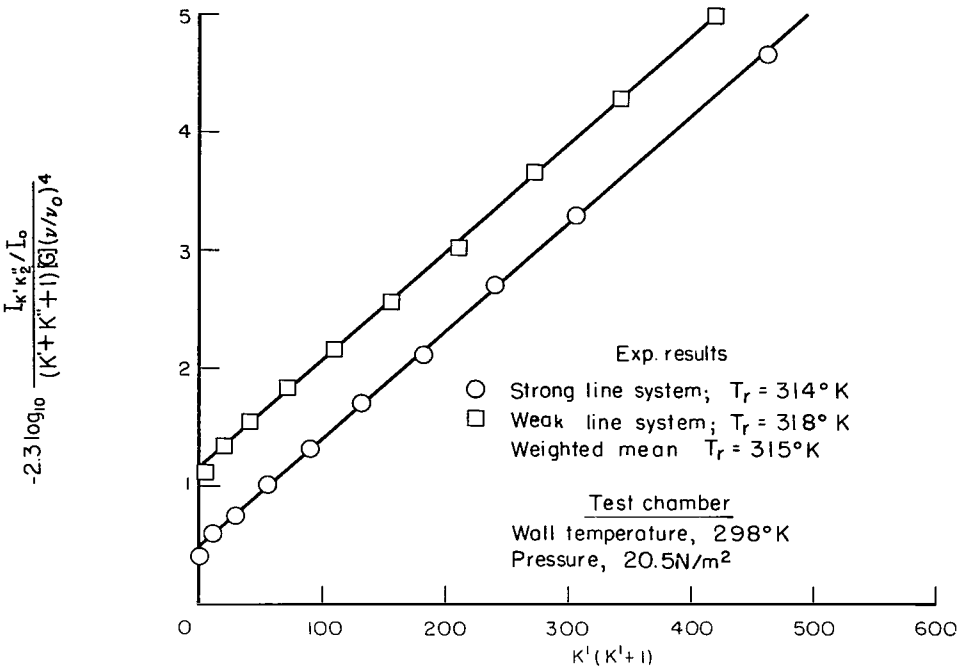

Figure 6.- $N_2^+(0,0)$ band data for 300° K experiment for T_r measurements.

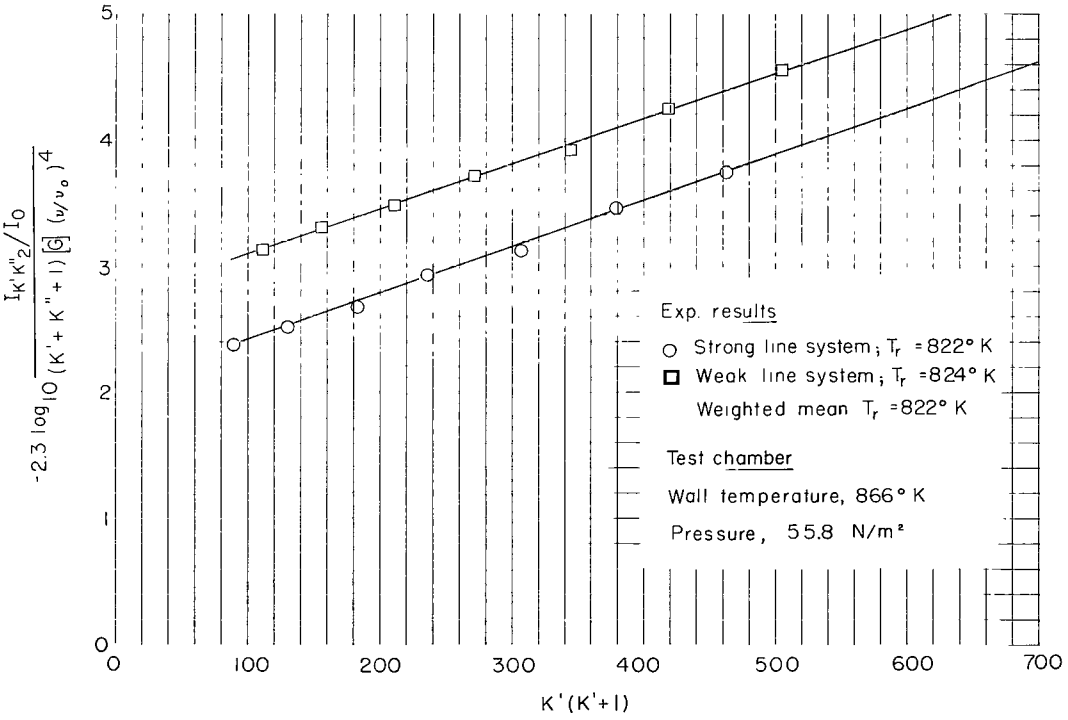

Figure 7.- $N_2^+(0,0)$ band data for 800° K experiment for T_r measurements.

with the standard deviation of each curve with respect to its best straight-line fit to the data points. It should be noted that the quantity $[G](\nu/\nu_0)^4$ (see table 1) is temperature dependent and that an iteration process is required in the determination of the rotational-temperature value.

The test data are given in figures 8 and 9 as plots of the percent difference between the weighted-mean value of the rotational temperatures and the gas temperature as a function of the gas temperature. The gas temperature is the wall temperature of the chamber corrected in accordance with figure 3. Two points should be noted. The first point is that the general trend of the data indicates a uniform variation in the percent difference between the measured weighted-mean value and the gas temperatures with increasing gas temperature up to approximately 1000° K. There are two data points in figure 8 at approximately 1050° K which do not follow this trend. This is attributed to the fact that equation (1) as originally derived is assumed to hold for temperatures up to 800° K (ref. 1) and, therefore, would not apply rigorously for higher gas temperatures. The second point is that the measured rotational temperature is high at ambient temperature and that the difference increased with an increase in gas number density. This result indicated

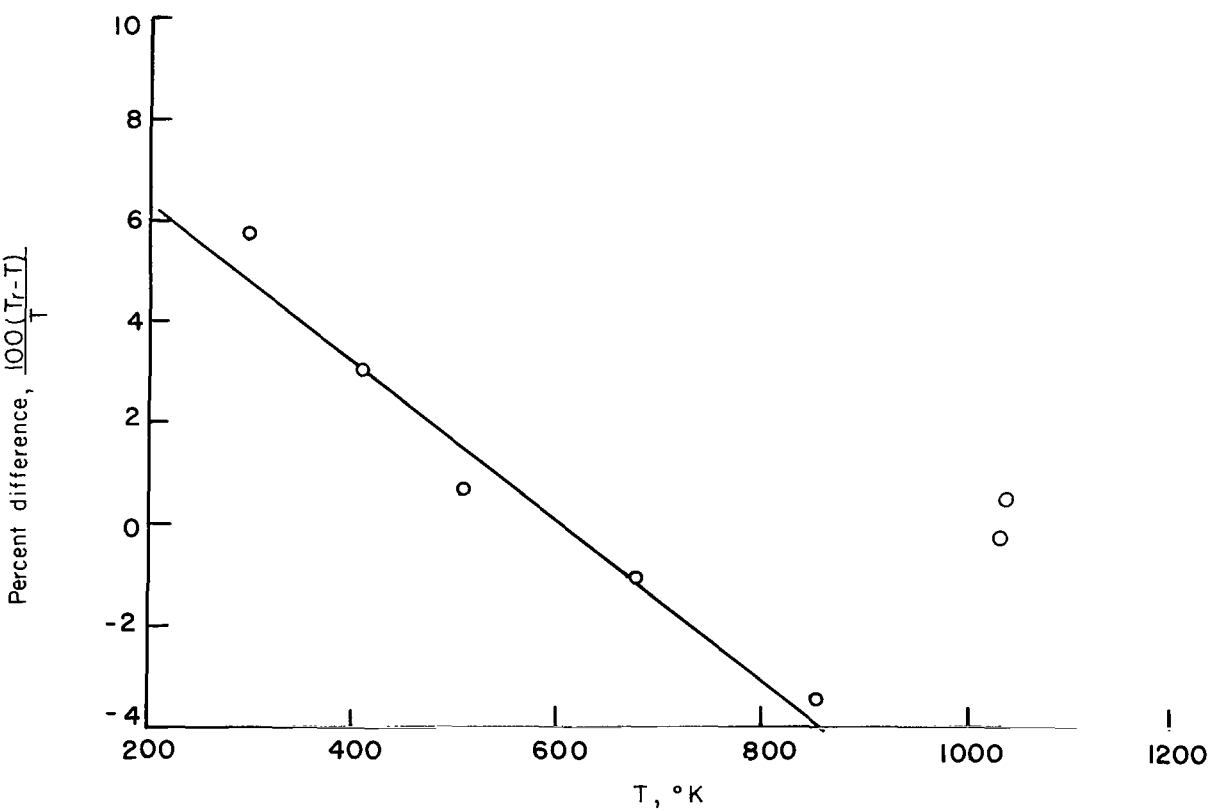

Figure 8.- Results of T_r tests for temperatures of 300° to 1000° K. Gas number density of 5×10^{15} cm^{-3}.

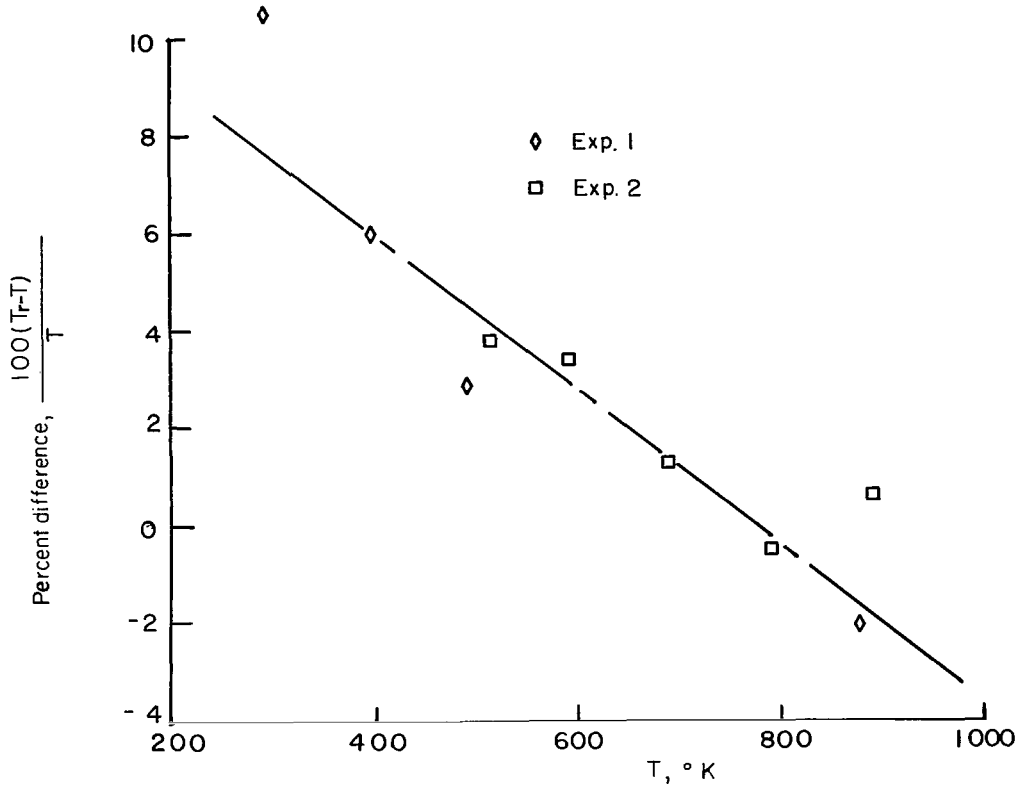

Figure 9.- Results of T_r tests for temperatures of 300^0 to 900^0 K. Gas number density of 1×10^{16} cm^{-3}.

that the measured rotational temperature was dependent on gas number density. Several investigators (refs. 1 and 4) have pointed out that T_r measurements made in a static gas were higher than the gas temperature.

Because of the preceding observations and results, tests were conducted to determine measured T_r dependence on the gas number density. All tests were conducted at ambient temperature which ranged from 287^0 to 303^0 K with an average of 291^0 K. The measured T_r was compared with the corresponding ambient temperature and plotted against the normalized number density as shown in figure 10. An analysis of the results provided the following empirical equation:

$$\Delta T = \log_{10}\left(\frac{n}{n_o}\right)^{15.7} \tag{2}$$

where ΔT is the difference between the gas temperature and the measured rotational temperature at the point of observation dependent on the number density n, and n_o is the reference gas number density arbitrarily selected as 3×10^{14} cm^{-3} because the results appear to intersect at this value for a unity ratio of T_r/T. The number density

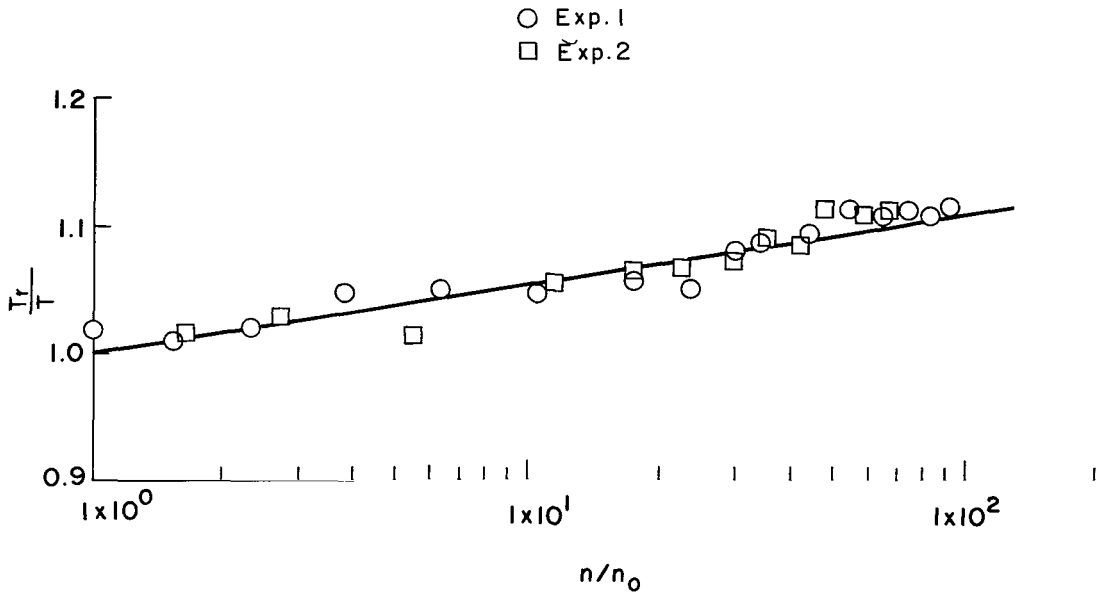

Figure 10.- Dependence of T_r on gas number density. $n_0 = 3 \times 10^{14}$ cm^{-3}.

n is limited to the range, 3×10^{14} cm$^{-3} \leq n \leq 3 \times 10^{16}$ cm^{-3}. On the basis of experimental observations, this increase in temperature is assumed to be a function of number density only and to be independent of gas temperature. Therefore, as the gas temperature increases, the change in T_r due to number density would become relatively small.

Equation (2) is assumed to be applicable to only the physical conditions of the tests reported herein. That is, effects of beam current, beam potential, and the distance of the observation point from the exit aperture of the electron gun were not included. All observations were made at a point 30 cm from the gun exit aperture, a beam current of 1100 μA, and a beam potential of 28.5 kV. The greater the distance from the aperture the greater will be the beam spreading for a given gas number density. If the gas heating should be dependent on the beam electron current density, spreading will be an important factor. It should be pointed out that changing the beam current by a factor of 2 did not change the measured T_r value within experimental precision. Also, the temperature of the gas at the point of observation is a function of a temperature gradient and, therefore, beam spreading again may be a factor because it could alter the gradient. However, until the exact molecular energy exchange mechanism or process is determined, tests should be conducted for each test configuration. The molecular heating mechanism must be determined in order to know conclusively the effects on the rotational temperature measurements in a flowing gas.

Tests similar to those of reference 4 were conducted with a dove prism. The dove prism was used to rotate the beam image so that it was perpendicular to the spectrometer

entrance slit. All other tests were conducted with the beam parallel to the entrance slit. The purpose of these tests was to obtain some quantitative information about the effects of secondary electrons by imaging the beam perpendicular to the entrance slit. Thereby, the fluorescence due to primary electrons was reduced and the fluorescence from the halo region about the beam center which is attributed to secondary electrons was increased. Within the experimental precision of this work, no difference was noted between T_r measurements taken with the beam image perpendicular and those taken with the beam image parallel to the entrance slit. This result did not permit any definite conclusions to be drawn about the effects of secondary electrons.

Results and Discussion

Corrections in accordance with equation (2) were applied to the measured rotational temperatures. The corrected results are shown in figure 11 which is a composite plot of data shown in figures 8 and 9. The resultant scatter of data has been reduced from +10 to -4 percent (figs. 8 and 9) to +2 to -6 percent (fig. 11). Also, the data are approximately grouped about a common curve. A slight difference in the data still exists for the two different densities. This difference can be attributed to the inaccuracy of equation (2)

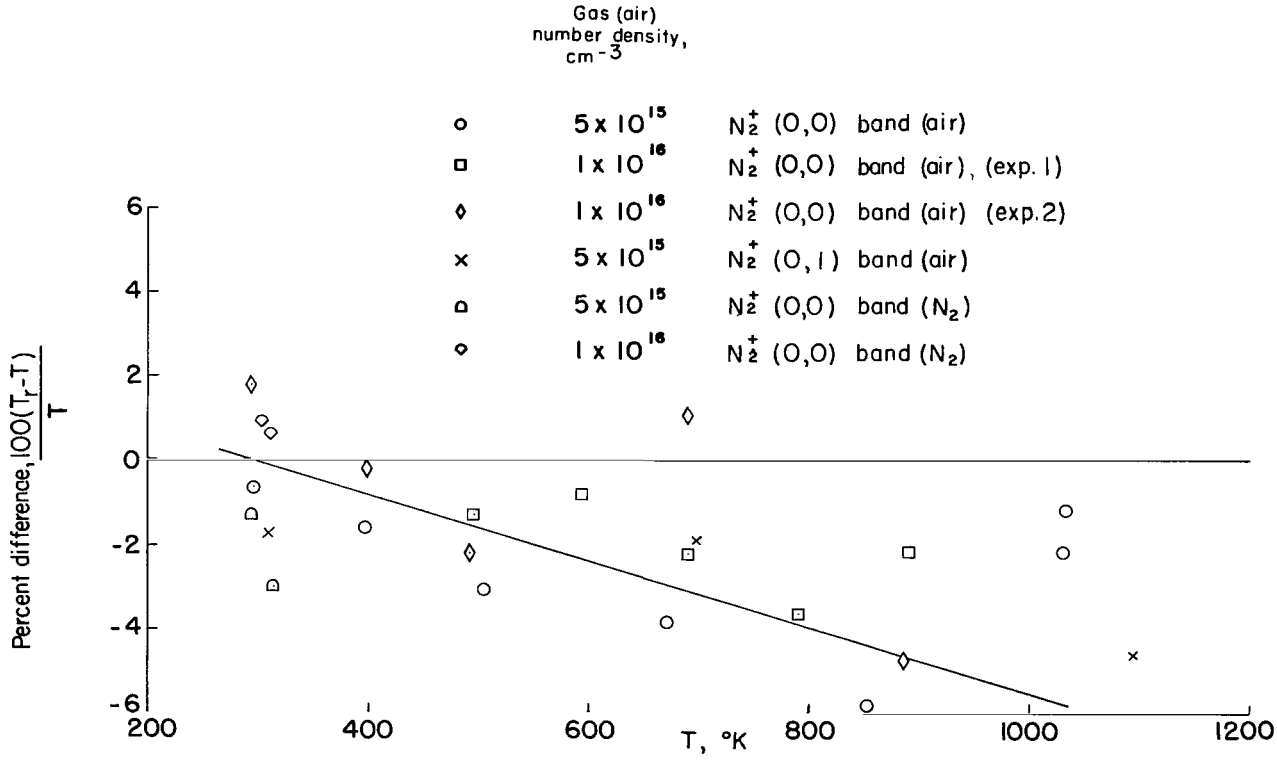

Figure 11.- Results of T_r tests corrected for gas-number-density effect for temperatures of 300^0 to 1000^0 K.

because of the experimental uncertainty associated with the data on which its derivation is based. The corrected results still indicate a slightly increasing difference between gas temperature and the measured rotational temperature. An analysis of equation (1) does not reveal any apparent sources of this difference. There are two possible causes. The first is possible experimental error. Careful analyses of all experimental apparatus have been made, and reasonable confidence has been established. The second possible source is found in the formulation of the theory leading to equation (1). The excitation-transition process is complex and no direct account of the effects of secondary-electron excitation processes has been made. Also, it was assumed that the rotational levels of the ground molecular state $N_2X^1\Sigma_g^+$ are in thermal equilibrium. Because a temperature difference does exist between the gas temperature and the measured rotational temperature, there will exist a population distribution of the rotational levels at the point of observation which is at least slightly non-Boltzmann (ref. 6). A slight deviation from a Boltzmann distribution would not be detected within the obtainable experimental precision but would affect the measured rotational-temperature value.

Additional T_r measurements were made in low-density nitrogen gas. The results of these measurements are shown in figure 11 for comparison with those measurements made from the nitrogen constituent of low-density air. There does not appear to be any significant difference between those measurements performed in air and those performed in nitrogen. This result is what would be expected because nitrogen is the primary constituent of air and collision quenching of the fluorescence of the first negative system of nitrogen by other constituents of air would not be a problem unless it was selective and greatly disturbed the relative molecular number density population of the excited state of nitrogen.

Rotational-temperature measurements were also made from the data obtained from the (0,1) band of N_2^+. The data reduction was performed in the identical manner described in the preceding sections. The values for $[G](\nu/\nu_0)^4$ used in equation (1) are given in table 2. The results are plotted in figure 11 for comparison with other results. No apparent difference exists between T_r measurements made from the (0,0) band data and those made from the (0,1) band data.

A relative precision of ±5 percent was estimated for these measurements. The factors affecting the relative precision of the measurements were the uncertainties in gas number density, gas temperature, and rotational temperature values obtained from the graphic solutions. A value of ±2 percent was calculated for the effects of density and gas temperature, and ±3 percent was estimated for the uncertainty of the measured temperature based on standard error values obtained from a large number of independent measurements.

VIBRATIONAL-TEMPERATURE MEASUREMENTS

Tests

The (0,1) and (1,2) bands of N_2^+ were selected for the vibrational-temperature measurements because there is no overlapping of second positive systems of N_2 at the test temperatures and because these bands are sufficiently intense to permit reasonably accurate intensity measurements. The test chamber was set to the desired temperature and a spectral trace, similar to that shown in figure 12, was obtained with a relatively wide spectrometer entrance slit. A slit width of 250 microns was used for these tests because it permitted sufficient instrument spectral resolution to distinguish the N_2^+ bands and provided a strong light level at the spectrometer photomultiplier cathode. The relative intensity of each band was determined by mechanically integrating the total area enclosed by each band envelope. For rotational temperatures greater than 400° K, it was necessary to correct the measured areas of each band because of the overlapping of the (0,1) band onto the (1,2) band. The relative intensity value, as determined from the spectral traces, was applied to the curve shown in figure 13, which is a plot of intensity ratio of the (0,1) band to the (1,2) band as a function of the vibrational temperature. This curve was calculated from the following equation:

$$\frac{I_{v_a' v_2''}}{I_{v_b' v_2''}} = \frac{\sum_{v_1''} e^{-E_{v_1''}/kT_v} P_{v_a' v_1''} A_{v_a' v_2''} \nu_{v_a' v_2''}}{\sum_{v_1''} e^{-E_{v_1''}/kT_v} P_{v_b' v_1''} A_{v_b' v_2''} \nu_{v_b' v_2''}} \tag{3}$$

The derivation of this equation and a general discussion of the theory leading to its derivation are given in the appendix. Tests were conducted for gas temperatures of approximately 300° K, 700° K, and 1100° K. The measured intensity ratios of the (0,1) band to (1,2) band are plotted against gas vibrational temperature in figure 13. The intensity ratios were corrected for variation in the spectral response of the detector which was determined from a calibration made with a standard lamp. The correction factor was 0.97.

Results and Discussion

Normally, when the electron beam technique is used, the vibrational temperature is not known. Therefore, the measured intensity ratio is plotted as a point on the curve in figure 13, and the corresponding temperature is determined. The precision of the

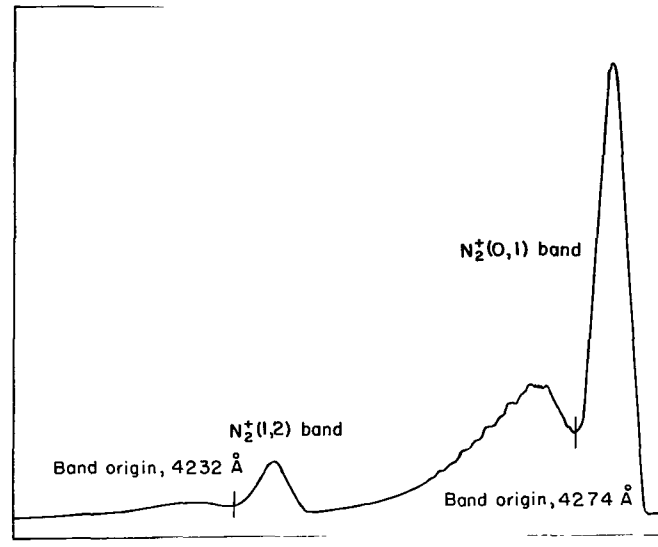

Figure 12.- Typical unresolved spectrometer trace of (0,1) and (1,2) bands of N_2^+. $T \approx 300^0$ K.

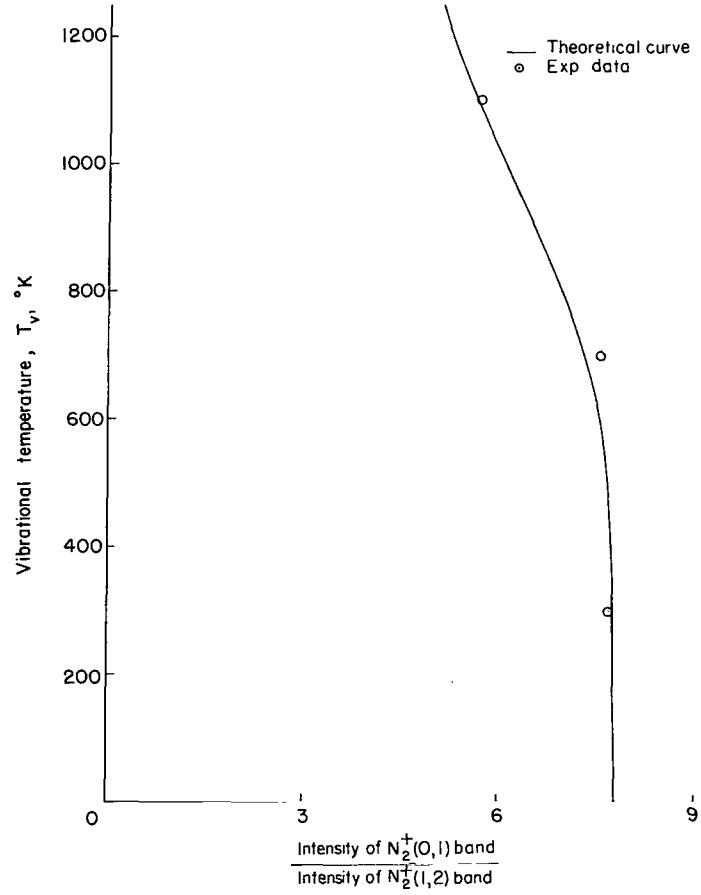

Figure 13.- Vibrational temperature as a function of intensity ratio of (0,1) band to (1,2) band of N_2^+.

measured temperature is determined by the precision of the measured intensity ratio. The main factor affecting this precision is the ability to account properly for the over lap of the (0,1) band onto the (1,2) band. For rotational temperatures below 400° K, accounting for the overlap is not a significant problem, but the limitation is the precision of the mechanics of measuring the area under the spectral envelope of each band. It is interesting to note that in hypersonic test facilities in which this technique can be applied, a nonequilibrium condition exists between rotational and vibrational energy states. This nonequilibrium condition is such that the rotational temperature is less than 400° K, but the vibrational temperatures are much greater. Therefore, a precise determination of intensity ratios can be made.

Another factor enters into the uncertainty of a vibrational temperature determined by this method. This factor is the accuracy of the transition probabilities used in determining the curve in figure 13 from equation (3). The accuracy of the transition probabilities is usually taken to be between 10 and 20 percent; a 15-percent value is taken for this work.

The total uncertainty of vibrational temperatures determined with this technique may be as large as 20 percent. The results of these tests show that this uncertainty is a fairly good estimate because the largest error was approximately 16 percent.

DISCUSSION OF RESULTS

Two significant results were noted in the work reported here. Neither result was predicted by the theoretical model developed by Muntz (ref. 1) for measuring rotational temperatures.

The first result is that the measured rotational temperature is a function of the gas number density. A theoretical explanation for this result is not known but it is apparent that there is an energy increase, or redistribution, in the rotational energy states of the molecules as the gas number density is increased. This increase or redistribution of energy could be a result of the excitation process. It is questionable whether this effect is due to the fast primary electrons, the lower energy secondaries, or both. However, Culp and Stair (ref. 7) recently performed experiments with low-energy (19- to 300-eV) electrons, which indicate that low-energy secondaries could be responsible. A portion of the secondary electrons is believed to lie in the energy range, $\geq$20 eV (ref. 8). The experimental results of Culp and Stair showed that the measured rotational temperature was a nonmonotonic function of the electron energy in the energy range of their investigation.

The second result is that the difference between the gas temperature and rotational temperature increases with an increase in gas temperature. The general trend of this

difference is indicated in figure 11 which shows that the rotational temperatures are lower than the gas temperatures. In order to obtain this result, it is necessary for the population of the lower rotational quantum states of $N_2^+X^2\Sigma_g^+$ to be enhanced or for the population of the upper quantum states to be decreased by some mechanism. The results of reference 4 appear to indicate a continuation of this trend in the low-temperature region, $\leq 300^\circ$ K, in which the rotational temperature is increasingly greater than the gas temperature for decreasing gas temperatures. This result is important because it indicates that some significant contribution to the excitation process is not accounted for in the present theory. It remains to be determined whether this result is due to a second-order effect which could be attributed to excitation by the fast primary electrons, to excitation by the secondary electrons, or to some other process.

Despite the differences noted in the preceding discussion, the present theory can be used for rotational-temperature measurements over the temperature range investigated with the expectation that the results will be within ± 10 percent of the true value. It is also believed that these results are pertinent to measurements performed in a flowing gas. To establish the relation between measurements in a static gas and those in a flowing gas, additional theoretical and experimental investigations are required. Therefore, it is essential to establish a theoretical description of the observed results and, on this basis, to ascertain the effects in a flowing gas.

CONCLUDING REMARKS

Laboratory measurements of rotational and vibrational temperatures have been performed over a range from 300° to 1100° K in static low-density air with an electron beam probe. The tests were conducted in a unique test chamber which permitted the selection of various combinations of test pressures and temperatures.

Rotational-temperature measurements were made from the (0,0) band of the first negative system of the nitrogen constituent of air. Some tests were also performed using the (0,1) band of the first negative system of nitrogen. No substantial differences were noted between the results of the (0,1) band tests and those of the (0,0) band tests.

The accuracy of the measured rotational temperatures was found to vary with gas temperature and gas number density. A difference existed between the measured rotational temperature and the gas temperature. This difference increased with increasing gas temperature. With the inclusion of an experimentally determined correction for the gas-number-density effect, the rotational-temperature measurements were made with an accuracy that varied from approximately +2 to -6 percent with increasing gas temperature.

Vibrational-temperature measurements were made by using the intensity ratios of the (0,1) and (1,2) bands of the first negative system of nitrogen. The measurements were found to be within ±20 percent of the gas temperature.

Langley Research Center,
National Aeronautics and Space Administration,
Langley Station, Hampton, Va., November 1, 1967,
125-24-03-22-23.

APPENDIX

THEORY

General

The test gas used in this investigation was air, and the primary sources of visible and near-ultraviolet radiation were the first negative and second positive systems of nitrogen. The excitation and emission path for the first negative system is illustrated by the energy-level diagram in figure 14. A high-energy electron, designated as a primary electron, is emitted by a source and has an inelastic collision with a ground-state nitrogen molecule, $N_2X^1\Sigma_g^+$. The molecule is excited to the excited ionized electronic state, $N_2^+B^2\Sigma_u^+$, from which it spontaneously radiates and drops into the ground energy state of the ion, $N_2^+X^2\Sigma_g^+$. The intensity and spectral distribution of the spontaneously emitted

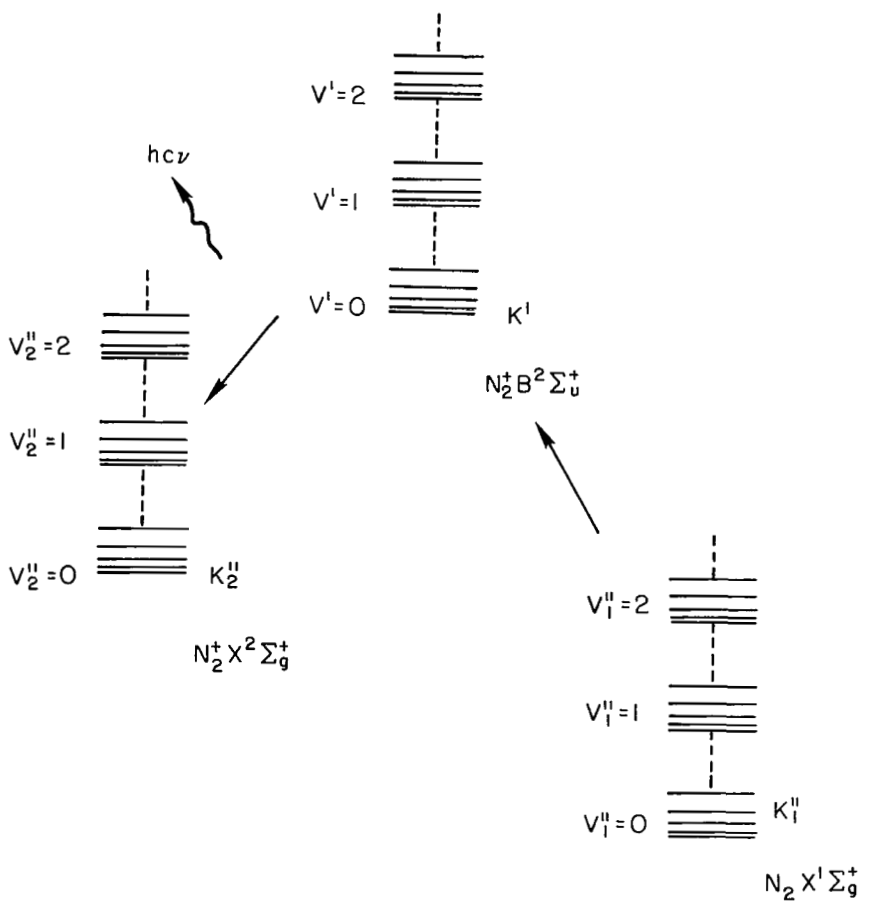

Figure 14.- Partial energy-level diagram of nitrogen.

radiation reflects the rotational and vibrational characteristics of the molecules that were in the $N_2X^1\Sigma_g^+$ state.

Rotational and vibrational temperatures may be obtained from an application of the intensity of emission equation

$$I_{nm} = N_n hc\nu_{nm}A_{nm} \tag{4}$$

where N_n is the number density population of the initial level of transition, $hc\nu_{nm}$ is the energy of the emitted radiation as a result of the transition between states n and m, ν_{nm} is the wave number of the emitted radiation, and A_{nm} is the transition probability of emission. All terms of equation (4) except N_n are constants or are dependent only on the particular transition involved. Application of equation (4) requires the determination of the population and its distribution in the initial electronic state, $N_2^+B^2\Sigma_u^+$.

On the basis of the arguments presented in reference 1, it is assumed that $N_2^+B^2\Sigma_u^+$ is populated primarily by neutral molecules in $N_2X^1\Sigma_g^+$. Population contributions from other possible origins are neglected. Therefore, the population of the rotational energy states of $N_2^+B^2\Sigma_u^+$ is determined by the excitation-transition process of $N_2X^1\Sigma_g^+$ molecules.

The excitation-transition process may be described through a Born-Oppenheimer approximation of the molecular wave function

$$\psi_{evJ\Lambda M} = \psi_e\left(\bar{r}_i, r_n\right)\frac{1}{r_n}\psi_v\left(r_n\right)\psi_{J\Lambda M}\left(\theta,\chi,\phi\right) \tag{5}$$

where ψ_e is the electronic wave function with the ith electronic coordinate $\bar{r}_i$ referenced to the molecular axis, ψ_v is the vibrational wave function with nuclei separation r_n, and $\psi_{J\Lambda M}$ is the rotational wave function which is a function of the Euler angles (θ,χ,ϕ). The Euler angles relate the molecular coordinate system to the coordinate system of the fixed point of observation. Also, it is assumed that the interaction of the primary electron with the orbital electrons can be described by a coulombic potential. Therefore, the following matrix element of this interaction may be used to describe the excitation:

$$\left(\hat{e}_p e_s B^2\Sigma_u^+ v'J'\Lambda'M'\left|\sum_i \frac{e^2}{r_{1i}}\right|e_p X^1\Sigma_g^+ v''J''\Lambda''M''\right) \tag{6}$$

In this expression, e_p and $\hat{e}_p$ represent the initial and final wave functions of the primary electrons, e_s represents the secondary electron, $X^1\Sigma_g^+$ and $B^2\Sigma_u^+$ represent the initial and final electronic wave functions, v'' and v' represent the vibrational

states, and $J''\Lambda''M''$ and $J'\Lambda'M'$ represent the rotational states. Of course, $\sum_i \frac{e^2}{r_{1i}}$ is the coulombic interaction term in which the quantity r_{1i} is the distance between the high-energy primary electron and the ith orbital electron.

Because the particular transition of interest results in the removal of one orbital electron, for simplicity $\sum_i \frac{1}{r_{1i}}$ will be replaced with $\frac{1}{r_{12}}$ where the subscript 2 denotes the removed electron. The electronic state $N_2^+B^2\Sigma_u^+$ is formed from the electronic state $N_2X^1\Sigma_g^+$ by the removal of a $\sigma_u 2s$ orbital electron (ref. 9). Therefore, the electronic state may be expressed as $X^1\Sigma_g^+ \equiv B^2\Sigma_u^+\sigma_u 2s$. Expression (6) is now rewritten as

$$\left(\hat{e}_p\hat{e}_s B^2\Sigma_u^+ v'K'\Lambda'M' \left| \frac{e^2}{r_{12}} \right| e_p\left[B^2\Sigma_u^+\sigma_u 2s\right] v''K''\Lambda''M''\right) \tag{7}$$

Note that K has been used in place of J. This substitution may be made by considering the applicable coupling scheme which is Hund's case (b) (ref. 9) and by suppressing the spin angular momentum.

In order to evaluate this matrix element for high-energy primary electrons, a plane-wave approximation is made for the primary-electron wave functions, and the integration over the primary-electron coordinates is performed. This integration gives (ref. 10)

$$\int \hat{e}_p(\bar{r}_1)\left(\frac{1}{r_{12}}\right)e_p(\bar{r}_1)d\bar{r}_1 = \frac{4\pi}{q^2} e^{i\bar{q}\cdot\bar{r}_2} \tag{8}$$

where $\bar{q}$ is the momentum transfer and $\bar{r}_2$ is the position vector of the interacting orbit electron. A series expansion of $e^{i\bar{q}\cdot\bar{r}_2}$ gives

$$e^{i\bar{q}\cdot\bar{r}_2} = 1 + i\bar{q}\cdot\bar{r}_2 - \frac{1}{2}\left(\bar{q}\cdot\bar{r}_2\right)^2 + \cdots \tag{9}$$

In a first-order approximation, the first two terms of this expansion are retained. But the contribution to the matrix element by the first term in equation (9) is zero because of the orthogonality of the initial and final states of the molecule. Therefore, equation (7) is given by

$$\frac{4\pi}{q^2} e^2\left(e_s B^2\Sigma_u^+ v'K'\Lambda'M' \left| i\bar{q}\cdot\bar{r}_2 \right| \left[B^2\Sigma_u^+\sigma_u 2s\right] v''K''\Lambda''M''\right) \tag{10}$$

APPENDIX

In order to evaluate expression (10) further, the vector $\bar{r}_2$ is transformed to the coordinates of the molecular axis through the dyadic $\bar{\bar{D}}(\theta,\chi,\phi)$ which relates the molecular coordinate axis to the fixed coordinate system of the point of observation. Therefore, expression (10) is rewritten as

$$\frac{i4\pi e^2\bar{q}}{q^2} \cdot \left(K'\Lambda'M'\left|\bar{\bar{D}}(\theta,\chi,\phi)\right|K''\Lambda''M''\right) \cdot \left(e_s B^2\Sigma_u^+ v'\left|\bar{r}_2^*\right|\left[B^2\Sigma_u^+\sigma_u 2s\right]v''\right) \tag{11}$$

where $\bar{r}_2^*$ is the position vector of the secondary electron with respect to the molecular axis. The square of the absolute value of the term $\frac{i4\pi e^2\bar{q}}{q^2}$ is contained in an excitation function C_e and will be suppressed in the following equations.

Evaluation of expression (11) shows that for $\Lambda' = \Lambda'' = 0$, $\Delta K = \pm 1$ transitions are allowed, whereas the $\Delta K = 0$ transition is forbidden, as assumed in reference 1. Also, further analysis of expression (10) in the form of expression (11) by using higher order terms of equation (9) indicates that transitions for $\Delta K = \pm 3$, $\Delta K = \pm 5$, and so forth, are also allowed. Of course, the magnitude of the cross sections for the excitation-transitions for $\Delta K = \pm 3$, $\Delta K = \pm 5$, and so forth, will determine the contribution to the population of the excited state. This contribution is expected to be small.

The square of the second matrix element in expression (11) is defined as the band strength or the vibrational transition probability and is designated $P_{v'v''}$. This band strength may be approximated by assuming a mean value of the internuclear separation and may then be written as

$$P_{v'v''} = \left|\left(e_s B^2\Sigma_u^+\left|\bar{r}_2^*\right|\left[B^2\Sigma_u^+\sigma_u 2s\right]\right)\right|^2 \left|(v'|v'')\right|^2 \tag{12}$$

The overlap integral of the vibrational wave functions squared $\left|(v'|v'')\right|^2$ is the Franck-Condon factor, $q_{v'v''}$. Generally, equation (12) is then expressed as

$$P_{v'v''} = \left|R_{ij}\right|^2 q_{v'v''} \tag{13}$$

In order to take into account the variation of internuclear separation, a method of $\bar{r}$ centroids (ref. 11) is used where $\bar{r}$ is the expectation value of the internuclear separation r_n as determined by the vibrational wave functions. Now, the band strength is given by

$$P_{v'v''} = \left|R_{ij}(r_n)\right|^2 q_{v'v''} \tag{14}$$

APPENDIX

The rotational-line strength is given by the square of the first matrix element of expression (11) summed over M'' and M'

$$\sum_{M'M''} \left| \left(K'\Lambda'M' \middle| \bar{\bar{D}} \middle| K''\Lambda''M'' \right) \right|^2 \tag{15}$$

This term is the Hönl-London factor, which is tabulated in reference 9. For the excitation transition of interest, which is indicated by the superscript a, the relative rotational-line strength may be obtained from the ratio of the line strength to the sum of the line strengths

$$P_R^a = \frac{S_{K''}^{K'}}{\sum_{K'} S_{K''}^{K'}} \tag{16}$$

The relative line strength for emission, designated P_R^e, is the same as that for excitation except that the summation is over K''.

The preceding work of this section has been based on a plane-wave approximation for the high-energy incident primary electron. It is also necessary to consider low-energy secondary electrons because they may contribute significantly to the number of ionized nitrogen molecules. Several observations may be made without making a detailed analysis of the excitation-transition process. For electronic states of the homonuclear nitrogen molecule, $X^1\Sigma_g^+$ and $B^2\Sigma_u^+$ rotational levels have symmetric and antisymmetric states under nuclear exchange. The symmetry properties of $X^1\Sigma_g^+$ and $B^2\Sigma_u^+$ are the opposite with respect to even and odd rotational quantum numbers, and only transitions between rotational energy levels with the same symmetry are allowed. Therefore, the selection rules with respect to ΔK which apply to high-energy electrons also apply to low-energy electrons. The only difficulty arises when the first-order approximation is not sufficiently accurate and $\Delta K = \pm 3$ or higher ΔK transitions are required to describe secondary-electron—induced transitions.

Vibrational Temperature

The intensity of spontaneously emitted radiation as a result of transitions between two vibrational energy states is given by

$$I_{v'v_2''} = N_{v'} hc \nu_{v'v_2''} A_{v'v_2''} \tag{17}$$

where $N_{v'}$ is the number density population of the initial vibrational level, $\nu_{v'v''_2}$ is the wave number of the resultant radiation of the transition, and $A_{v'v''_2}$ is the transition probability of spontaneous emission for transitions between the initial vibrational level v' and a terminal vibrational level v''_2.

For this work, it is assumed that $N_2X^1\Sigma_g^+$ is the primary source of molecules which are excited to $N_2^+B^2\Sigma_u^+$ as a result of inelastic electron collisions. Therefore, $N_{v'}$ and the resultant intensity of spontaneous emission are dependent on the distribution and the number density population of the vibrational energy states, $N_{v''_1}$, of $N_2X^1\Sigma_g^+$. The steady-state relation between $N_{v'}$ and $N_{v''_1}$ as a result of inelastic electron-N_2 collision is given by

$$N_{v'} = \frac{C_e}{R} \sum_{v''_1} N_{v''_1} P_{v'v''_1} \tag{18}$$

where the product $C_e \sum_{v''_1} P_{v'v''_1}$ describes the excitation and transition process between v''_1 and v'. The term C_e is an excitation function, $P_{v'v''_1}$ is the vibrational band strength described in the preceding section, and R is the depopulation rate. The term C_e/R will be designated $\hat{C}_e$ henceforth. If it is assumed that the $N_2X^1\Sigma_g^+$ vibrational energy states are in thermal equilibrium, the number of molecules in a given $N_{v''_1}$ vibrational state is given by a Boltzmann distribution

$$N_{v''_1} = \frac{N_o}{Q_v} e^{-E_{v''_1}/kT_v} \tag{19}$$

where $Q_v = \sum_{v''_1} e^{-E_{v''_1}/kT_v}$ is the "state sum" or partition function, $E_{v''_1} = G_o(v''_1)hc$ is the characteristic energy of the v''_1 level, $G_o(v''_1)$ is the vibrational term, N_o is the steady-state population of $N_2X^1\Sigma_g^+$, and T_v is the vibrational temperature. Therefore, with the substitution of equation (19) into equation (18), the dependence of $N_{v'}$ on the T_v of $N_2X^1\Sigma_g^+$ is established, and the relation between the vibrational temperature of $N_2X^1\Sigma_g^+$ and the intensity of spontaneously emitted radiation (eq. (16)) can be determined.

It is not necessary to make absolute-intensity measurements because T_v may be determined from the ratio of intensities of two vibrational bands. The resultant equation, as derived from equations (17), (18), and (19), is

APPENDIX

$$\frac{I_{v'_a v''_2}}{I_{v'_b v''_2}} = \frac{\sum_{v''_1} e^{-E_{v''_1}/kT_v} P_{v'_a v''_1} A_{v'_a v''_2} \nu_{v'_a v''_2}}{\sum_{v''_1} e^{-E_{v''_1}/kT_v} P_{v'_b v''_1} A_{v'_b v''_2} \nu_{v'_b v''_2}} \tag{20}$$

Note that C_e, N_o, and Q_v canceled in the preceding ratio because these terms are independent of a particular v', v''_1 transition. Therefore, with equation (20), the variation of the intensity ratio as a function of T_v may be calculated. As an example, the calculation for the intensity ratio for the (0,1) to (1,2) bands is shown in figure 13. The transition probabilities used for this example were obtained from references 12 and 13.

Rotational Temperature

The rotational number density, $N_{K'}$, of $N_2^+ B^2\Sigma_u^+$ is a function of the excitation-transition process, depopulation rate, and number density, $N_{K''_1}$, of $N_2 X^1\Sigma_g^+$. If it is assumed that rotational states of v''_1 are in thermal equilibrium, $N_{K''_1}$ is given by (ref. 9)

$$N_{K''_1} = \frac{N_{v''_1}}{Q_r}\left(2K''_1 + 1\right) e^{-E_{K''_1}/kT_r} \tag{21}$$

where $Q_r = \sum_{K''} \left(2K'' + 1\right) e^{-E_{K''_1}/kT_r}$ is the rotational partition function, $E_{K''_1} = F\left(K''_1\right)hc$ is the characteristic energy of a rotational state, $F\left(K''_1\right)$ is the rotational term, and T_r is the rotational temperature. A relation to a temperature has been established through the Boltzmann factor which explicitly assumes that thermal equilibrium exists in the ground electronic state of the neutral species of N_2.

In order to interpret this temperature dependence in the resulting intensity of radiation, the selection rules for transitions between various rotational energy states are applied. As a first approximation, the applicable selection rule for the excitation-transition process is taken to be $\Delta K = \pm 1$. The $\Delta K = \pm 1$ selection rule predicts the formation of a P branch and R branch in the rotational fine structure of a vibrational band in excitation as well as emission. Figure 15 shows the R and P branches of the (0,0) band of N_2^+.

The following derivation is similar to that of reference 1 by E. P. Muntz. With the formation of the P and R branches, the steady-state population of $N_2^+ B^2\Sigma_u^+$ is given by

APPENDIX

$$N_{K'} = \hat{C}_e \sum_{v_1''} \left\{ \left[N_{K_1''-1} P^a_{RR} + N_{K_1''+1} P^a_{RP} \right] \cdot P_{v'v_1''} \right\} \tag{22}$$

where P^a_{RR} and P^a_{RP} are the relative rotational-line strengths of absorption, previously described, for the P and R branches.

With the determination of $N_{K'}$, the intensity of emitted radiation may be calculated as a function of the rotational temperature T_r. Before the calculation may be accomplished, it is necessary to set up an expression for the emission transition probability $A_{K'K_2''}$ as

$$A_{K'K_2''} = X\nu^3 P_{v'v_2''} P^e_R \tag{23}$$

where X is a constant, ν is the wave number of the transition, and P^e_R is the relative rotational transition probability for emission.

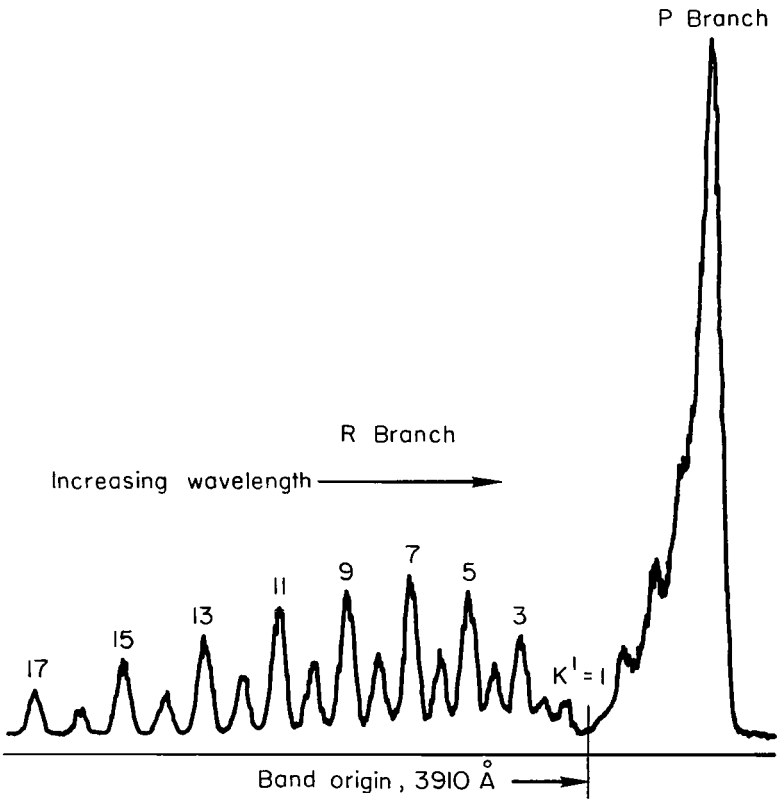

Figure 15.- Spectrometer trace of rotational structure of $N_2^+(0,0)$ band. $T \approx 300^\circ$ K.

APPENDIX

The intensity of emission for a particular R-branch transition is given by

$$I_{K'K''_2} = X\hat{C}_e\nu^4 \sum_{v''_1} \left[\frac{\frac{N_o}{Q_v} e^{-E_{v''_1}/kT_v} P_{v'v''_1}(A)}{Q_r} \right] \left(\frac{K'}{2K' + 1} \right) P_{v'v''_2} \tag{24}$$

where

$$(A) = K' e^{-E_{K'-1}/kT_r} + (K' + 1) e^{-E_{K'+1}/kT_r} \tag{25}$$

This equation is simplified by noting that the product

$$X\hat{C}_e P_{v'v''_2} N_o / Q_v = W \tag{26}$$

where W is a constant for a particular (v', v''_2) transition. Also, the equation may be put in conventional form (ref. 9) by noting that $2K' = K' + K''_2 + 1$ for R-branch transitions. Therefore,

$$\frac{I_{K'K''_2}}{K' + K''_2 + 1} = \frac{W\nu^4}{2(2K' + 1)} \sum_{v''_1} \frac{P_{v'v''_1} e^{-E_{v''_1}/kT_v} (A)}{Q_r} \tag{27}$$

For $T_v \leqq 800^o$ K, 99 percent of the total population is in the $v''_1 = 0$ level. Equation (24) may now be written

$$\frac{I_{K'K''_2}/I_o}{K' + K''_2 + 1} = Y\nu^4 [G] e^{-B_0 K'(K'+1)hc/kT_r} \tag{28}$$

where B_0 is the rotational constant related to the $v''_1 = 0$ vibrational level of $N_2 X^1\Sigma_g^+$,

$$Y = \frac{W P_{v'v''_1} e^{-E_{v''_1}/kT_v}}{2Q_r I_o} \tag{29}$$

and

APPENDIX

$$[G] = \frac{K' e^{2B_0 K' hc/kT_r} + (K' + 1) e^{-2B_0(K'+1)hc/kT_r}}{2K' + 1} \tag{30}$$

Note that a reference intensity I_o has been included to permit the measurements of relative intensities. The term $[G]$ involves T_r and requires a solution of equation (21) through a process of iteration.

Analysis of equation (27) also reveals that only a small error ($\approx \pm 1$ percent) will be introduced by extending the application of equation (28) to the temperature of 1000° K. This analysis was performed by calculating an effective value for rotational constant to replace B_0 in equation (28).

For ease of application, equation (28) is put in the following form:

$$\frac{B_0 hc}{kT_r} K'(K' + 1) + Z = -2.3 \log_{10} \frac{I_{K'K_2''}/I_o}{\left(K' + K_2'' + 1\right)\left[[G]\left(\nu/\nu_o\right)^4\right]} \tag{31}$$

where ν_o is a reference wave number used to normalize ν. From reference 1, the ν_o value is chosen for the (3,2) transition. Also, Z is just $-2.3 \log_{10} Y$, which is a constant.

REFERENCES

1. Muntz, E. P.: Static Temperature Measurements in a Flowing Gas. Phys. Fluids, vol. 5, no. 1, Jan. 1962, pp. 80-90.

2. Sebacher, Daniel I.; and Duckett, Roy J.: A Spectrographic Analysis of a 1-Foot Hypersonic-Arc-Tunnel Airstream Using an Electron Beam Probe. NASA TR R-214, 1964.

3. Petrie, S. L.; Pierce, G. A.; and Fishburne, E. S.: Analysis of the Thermo-Chemical State of an Expanded Air Plasma. Tech. Rept. No. AFFDL-TR-64-191, Ohio State Univ. Res. Found., Aug. 1965.

4. Robben, F.; and Talbot, L.: Measurements of Rotational Temperatures in a Low Density Wind Tunnel. Phys. Fluids, vol. 9, no. 4, Apr. 1966, pp. 644-652.

5. Muntz, E. P.; and Abel, Shirley J.: The Direct Measurement of Static Temperatures in Stock Tunnel Flows. Third Hypervelocity Techniques Symposium, Univ. of Denver and Arnold Eng. Develop. Center, Mar. 1964, pp. 51-87.

6. Kennard, Earle H.: Kinetic Theory of Gases. McGraw-Hill Book Co., Inc., 1938.

7. Culp, G.; and Stair, A. T., Jr.: Effective Rotational Temperatures of N_2^+ (3914 Å) Excited by Monoenergetic Electrons in a Crossed Beam. J. Chim. Phys., t. 64, no. 1, Jan. 1967, pp. 57-62.

8. Muntz, E. P.; and Marsden, D. J.: Electron Excitation Applied to the Experimental Investigation of Rarefied Gas Flows. Rarefied Gas Dynamics, Vol. II, J. A. Laurmann, ed., Academic Press, 1963, pp. 495-526.

9. Herzberg, Gerhard: Molecular Spectra and Molecular Structure. I. Spectra of Diatomic Molecules. Second ed., D. Van Nostrand Co., Inc., c.1950.

10. Landau, L. D.; and Lifshitz, E. M. (J. B. Sykes and J. S. Bell, trans.): Quantum Mechanics – Non-Relativistic Theory. Volume 3 of Course of Theoretical Physics, Addison-Wesley Pub. Co., Inc., c.1958.

11. Fraser, P. A.: A Method of Determining the Electronic Transition Moment for Diatomic Molecules. Can. J. Phys., vol. 32, no. 8, Aug. 1954, pp. 515-521.

12. Bates, D. R.: The Intensity Distribution in the Nitrogen Band Systems Emitted From the Earth's Upper Atmosphere. Proc. Roy. Soc. (London), ser. A, vol. 196, Mar. 1949, pp. 217-250.

13. Wallace, L. V.; and Nicholls, R. W.: The Interpretation of Intensity Distributions in the N_2 Second Positive and N_2^+ First Negative Band Systems. J. Atmospheric Terrest. Phys. (Res. Notes), vol. 7, nos. 1/2, Aug. 1955, pp. 101-105.

TABLE I.- $\log_{10} [G](\nu/\nu_0)^4$ VALUES FOR (0,0) BAND.

K' \ T_r	50.0	75.0	100.0	125.0	150.0	175.0	200.0	225.0	250.0	275.0	300.0	325.0	350.0	400.0
0	-0.0507	-0.0341	-0.0258	-0.0208	-0.0175	-0.0151	-0.0133	-0.0120	-0.0109	-0.0099	-0.0092	-0.0086	-0.0080	-0.0071
1	-0.0445	-0.0312	-0.0241	-0.0196	-0.0166	-0.0144	-0.0127	-0.0114	-0.0103	-0.0095	-0.0088	-0.0081	-0.0076	-0.0068
2	-0.0325	-0.0257	-0.0208	-0.0174	-0.0150	-0.0131	-0.0117	-0.0105	-0.0096	-0.0088	-0.0081	-0.0076	-0.0071	-0.0063
3	-0.0152	-0.0178	-0.0162	-0.0144	-0.0127	-0.0114	-0.0103	-0.0094	-0.0086	-0.0079	-0.0073	-0.0068	-0.0064	-0.0057
4	0.0073	-0.0073	-0.0102	-0.0104	-0.0099	-0.0092	-0.0085	-0.0079	-0.0073	-0.0068	-0.0064	-0.0060	-0.0056	-0.0050
5	0.0343	0.0054	-0.0027	-0.0054	-0.0063	-0.0065	-0.0064	-0.0061	-0.0058	-0.0055	-0.0052	-0.0049	-0.0046	-0.0042
6	0.0653	0.0203	0.0060	0.0004	-0.0022	-0.0033	-0.0038	-0.0040	-0.0040	-0.0040	-0.0039	-0.0037	-0.0036	-0.0032
7	0.0998	0.0373	0.0161	0.0070	0.0026	0.0003	-0.0010	-0.0017	-0.0021	-0.0023	-0.0024	-0.0024	-0.0023	-0.0022
8	0.1372	0.0562	0.0274	0.0145	0.0080	0.0044	0.0023	0.0010	0.0002	-0.0003	-0.0007	-0.0009	-0.0010	-0.0011
9	0.1772	0.0769	0.0398	0.0229	0.0140	0.0090	0.0059	0.0040	0.0027	0.0018	0.0012	0.0008	0.0005	0.0002
10	0.2192	0.0991	0.0533	0.0320	0.0206	0.0140	0.0099	0.0072	0.0054	0.0041	0.0032	0.0026	0.0021	0.0015
11	0.2630	0.1228	0.0679	0.0418	0.0278	0.0194	0.0142	0.0107	0.0084	0.0067	0.0055	0.0046	0.0039	0.0030
12	0.3081	0.1477	0.0835	0.0524	0.0354	0.0253	0.0188	0.0145	0.0115	0.0094	0.0078	0.0067	0.0058	0.0045
13	0.3544	0.1739	0.1000	0.0638	0.0437	0.0316	0.0239	0.0186	0.0150	0.0124	0.0104	0.0089	0.0078	0.0062
14	0.4016	0.2010	0.1173	0.0757	0.0524	0.0383	0.0292	0.0230	0.0186	0.0155	0.0131	0.0113	0.0100	0.0080
15	0.4496	0.2291	0.1355	0.0883	0.0617	0.0454	0.0348	0.0276	0.0225	0.0188	0.0160	0.0139	0.0122	0.0099
16	0.4981	0.2580	0.1543	0.1015	0.0714	0.0529	0.0408	0.0325	0.0266	0.0223	0.0191	0.0166	0.0147	0.0119
17	0.5471	0.2876	0.1738	0.1152	0.0816	0.0607	0.0471	0.0377	0.0309	0.0260	0.0223	0.0194	0.0172	0.0140
18	0.5965	0.3177	0.1940	0.1295	0.0922	0.0690	0.0536	0.0431	0.0355	0.0299	0.0257	0.0224	0.0199	0.0162
19	0.6462	0.3485	0.2147	0.1443	0.1032	0.0775	0.0605	0.0487	0.0402	0.0340	0.0292	0.0256	0.0227	0.0185
20	0.6961	0.3797	0.2359	0.1595	0.1147	0.0864	0.0677	0.0546	0.0452	0.0382	0.0329	0.0288	0.0256	0.0209
21	0.7462	0.4113	0.2576	0.1752	0.1265	0.0957	0.0751	0.0607	0.0504	0.0427	0.0368	0.0323	0.0287	0.0234
22	0.7964	0.4433	0.2797	0.1913	0.1387	0.1052	0.0828	0.0671	0.0557	0.0473	0.0408	0.0358	0.0318	0.0260
23	0.8468	0.4756	0.3022	0.2077	0.1512	0.1151	0.0908	0.0737	0.0613	0.0521	0.0450	0.0395	0.0351	0.0287

K' \ T_r	450.0	500.0	550.0	600.0	650.0	700.0	750.0	800.0	850.0	900.0	950.0	1000.0	1050.0	1100.0
0	-0.0064	-0.0059	-0.0054	-0.0050	-0.0047	-0.0045	-0.0042	-0.0040	-0.0038	-0.0037	-0.0035	-0.0034	-0.0033	-0.0032
1	-0.0061	-0.0055	-0.0051	-0.0047	-0.0044	-0.0042	-0.0039	-0.0037	-0.0035	-0.0034	-0.0032	-0.0031	-0.0030	-0.0029
2	-0.0056	-0.0051	-0.0047	-0.0043	-0.0040	-0.0038	-0.0036	-0.0034	-0.0032	-0.0030	-0.0029	-0.0028	-0.0026	-0.0025
3	-0.0051	-0.0046	-0.0042	-0.0039	-0.0036	-0.0034	-0.0032	-0.0030	-0.0028	-0.0027	-0.0025	-0.0024	-0.0023	-0.0022
4	-0.0045	-0.0041	-0.0037	-0.0034	-0.0031	-0.0029	-0.0027	-0.0025	-0.0024	-0.0022	-0.0021	-0.0020	-0.0019	-0.0018
5	-0.0038	-0.0034	-0.0031	-0.0028	-0.0026	-0.0024	-0.0022	-0.0021	-0.0019	-0.0018	-0.0017	-0.0016	-0.0015	-0.0014
6	-0.0030	-0.0027	-0.0024	-0.0022	-0.0020	-0.0018	-0.0017	-0.0015	-0.0014	-0.0013	-0.0012	-0.0011	-0.0010	-0.0009
7	-0.0021	-0.0019	-0.0017	-0.0015	-0.0014	-0.0012	-0.0011	-0.0010	-0.0009	-0.0008	-0.0007	-0.0006	-0.0005	-0.0004
8	-0.0011	-0.0010	-0.0009	-0.0008	-0.0007	-0.0006	-0.0005	-0.0004	-0.0003	-0.0002	-0.0001	-0.0000	0.0000	0.0001
9	0.0000	-0.0000	-0.0000	-0.0000	0.0001	0.0001	0.0002	0.0003	0.0003	0.0004	0.0005	0.0005	0.0006	0.0006
10	0.0012	0.0010	0.0009	0.0009	0.0009	0.0009	0.0009	0.0009	0.0010	0.0010	0.0011	0.0011	0.0012	0.0012
11	0.0024	0.0021	0.0019	0.0018	0.0017	0.0017	0.0017	0.0017	0.0017	0.0017	0.0017	0.0018	0.0018	0.0018
12	0.0038	0.0033	0.0030	0.0028	0.0026	0.0025	0.0025	0.0024	0.0024	0.0024	0.0024	0.0024	0.0025	0.0025
13	0.0052	0.0046	0.0041	0.0038	0.0036	0.0034	0.0033	0.0033	0.0032	0.0032	0.0032	0.0032	0.0032	0.0032
14	0.0067	0.0059	0.0053	0.0049	0.0046	0.0044	0.0042	0.0041	0.0040	0.0040	0.0039	0.0039	0.0039	0.0039
15	0.0084	0.0073	0.0066	0.0061	0.0057	0.0054	0.0052	0.0050	0.0049	0.0048	0.0047	0.0047	0.0046	0.0046
16	0.0101	0.0088	0.0079	0.0073	0.0068	0.0065	0.0062	0.0060	0.0058	0.0057	0.0056	0.0055	0.0054	0.0054
17	0.0119	0.0104	0.0093	0.0086	0.0080	0.0076	0.0072	0.0070	0.0067	0.0066	0.0065	0.0064	0.0063	0.0062
18	0.0137	0.0120	0.0108	0.0099	0.0092	0.0087	0.0083	0.0080	0.0077	0.0075	0.0074	0.0072	0.0071	0.0070
19	0.0157	0.0137	0.0123	0.0113	0.0105	0.0099	0.0094	0.0091	0.0088	0.0085	0.0083	0.0082	0.0080	0.0079
20	0.0177	0.0155	0.0139	0.0127	0.0118	0.0111	0.0106	0.0102	0.0098	0.0095	0.0093	0.0091	0.0089	0.0088
21	0.0199	0.0174	0.0156	0.0142	0.0132	0.0124	0.0118	0.0113	0.0109	0.0106	0.0103	0.0101	0.0099	0.0097
22	0.0221	0.0193	0.0173	0.0158	0.0147	0.0138	0.0131	0.0125	0.0120	0.0117	0.0114	0.0111	0.0109	0.0107
23	0.0244	0.0213	0.0191	0.0174	0.0162	0.0152	0.0144	0.0137	0.0132	0.0128	0.0125	0.0122	0.0119	0.0117

TABLE 2.- $\log_{10}[G](\nu/\nu_0)^4$ VALUES FOR (0,1) BAND.

K' \ T_r	50.0	75.0	100.0	125.0	150.0	175.0	200.0	225.0	250.0	275.0	300.0	325.0	350.0	400.0
0	-0.0507	-0.0342	-0.0259	-0.0209	-0.0176	-0.0152	-0.0134	-0.0120	-0.0109	-0.0100	-0.0093	-0.0086	-0.0081	-0.0072
1	-0.0446	-0.0313	-0.0241	-0.0197	-0.0166	-0.0144	-0.0128	-0.0115	-0.0104	-0.0096	-0.0088	-0.0082	-0.0077	-0.0068
2	-0.0326	-0.0258	-0.0209	-0.0175	-0.0150	-0.0132	-0.0117	-0.0106	-0.0096	-0.0088	-0.0082	-0.0076	-0.0071	-0.0063
3	-0.0152	-0.0178	-0.0162	-0.0144	-0.0127	-0.0114	-0.0103	-0.0094	-0.0086	-0.0079	-0.0073	-0.0068	-0.0064	-0.0057
4	0.0073	-0.0073	-0.0101	-0.0103	-0.0098	-0.0091	-0.0085	-0.0078	-0.0073	-0.0068	-0.0063	-0.0059	-0.0056	-0.0049
5	0.0344	0.0055	-0.0026	-0.0054	-0.0062	-0.0064	-0.0063	-0.0060	-0.0057	-0.0054	-0.0051	-0.0048	-0.0046	-0.0041
6	0.0654	0.0205	0.0062	0.0005	-0.0020	-0.0032	-0.0037	-0.0039	-0.0039	-0.0038	-0.0037	-0.0036	-0.0034	-0.0031
7	0.0999	0.0375	0.0163	0.0072	0.0028	0.0005	-0.0008	-0.0015	-0.0019	-0.0021	-0.0022	-0.0022	-0.0022	-0.0020
8	0.1375	0.0565	0.0276	0.0148	0.0083	0.0047	0.0026	0.0013	0.0004	-0.0001	-0.0004	-0.0006	-0.0007	-0.0008
9	0.1775	0.0772	0.0401	0.0232	0.0144	0.0093	0.0062	0.0043	0.0030	0.0021	0.0015	0.0011	0.0008	0.0005
10	0.2196	0.0995	0.0537	0.0324	0.0210	0.0144	0.0103	0.0076	0.0058	0.0045	0.0036	0.0030	0.0025	0.0019
11	0.2635	0.1232	0.0684	0.0423	0.0282	0.0199	0.0147	0.0112	0.0088	0.0071	0.0059	0.0050	0.0043	0.0034
12	0.3087	0.1483	0.0841	0.0530	0.0360	0.0259	0.0194	0.0151	0.0121	0.0100	0.0084	0.0072	0.0063	0.0051
13	0.3551	0.1745	0.1006	0.0644	0.0443	0.0322	0.0245	0.0193	0.0156	0.0130	0.0110	0.0096	0.0084	0.0069
14	0.4024	0.2018	0.1181	0.0764	0.0532	0.0390	0.0299	0.0237	0.0194	0.0162	0.0138	0.0121	0.0107	0.0087
15	0.4504	0.2299	0.1363	0.0891	0.0625	0.0462	0.0356	0.0284	0.0233	0.0196	0.0168	0.0147	0.0131	0.0107
16	0.4990	0.2588	0.1552	0.1023	0.0723	0.0538	0.0417	0.0334	0.0275	0.0232	0.0199	0.0175	0.0155	0.0128
17	0.5481	0.2886	0.1749	0.1162	0.0826	0.0618	0.0481	0.0387	0.0320	0.0270	0.0233	0.0205	0.0182	0.0150
18	0.5976	0.3189	0.1951	0.1306	0.0933	0.0701	0.0548	0.0442	0.0366	0.0310	0.0268	0.0236	0.0210	0.0173
19	0.6474	0.3497	0.2159	0.1455	0.1045	0.0788	0.0617	0.0499	0.0415	0.0352	0.0305	0.0268	0.0239	0.0197
20	0.6974	0.3811	0.2372	0.1608	0.1160	0.0878	0.0690	0.0560	0.0466	0.0396	0.0343	0.0302	0.0270	0.0223
21	0.7476	0.4128	0.2590	0.1766	0.1280	0.0972	0.0766	0.0622	0.0518	0.0441	0.0383	0.0337	0.0301	0.0249
22	0.7980	0.4449	0.2813	0.1929	0.1403	0.1069	0.0844	0.0687	0.0573	0.0489	0.0424	0.0374	0.0334	0.0276
23	0.8485	0.4773	0.3039	0.2095	0.1530	0.1168	0.0925	0.0754	0.0630	0.0538	0.0467	0.0412	0.0369	0.0305

K' \ T_r	450.0	500.0	550.0	600.0	650.0	700.0	750.0	800.0	850.0	900.0	950.0	1000.0	1050.0	1100.0
0	-0.0065	-0.0060	-0.0055	-0.0051	-0.0048	-0.0045	-0.0043	-0.0041	-0.0039	-0.0038	-0.0036	-0.0035	-0.0034	-0.0033
1	-0.0062	-0.0056	-0.0052	-0.0048	-0.0045	-0.0042	-0.0040	-0.0038	-0.0036	-0.0034	-0.0033	-0.0032	-0.0031	-0.0029
2	-0.0057	-0.0052	-0.0047	-0.0044	-0.0041	-0.0038	-0.0036	-0.0034	-0.0032	-0.0031	-0.0029	-0.0028	-0.0027	-0.0026
3	-0.0051	-0.0046	-0.0042	-0.0039	-0.0036	-0.0034	-0.0032	-0.0030	-0.0028	-0.0027	-0.0025	-0.0024	-0.0023	-0.0022
4	-0.0044	-0.0040	-0.0037	-0.0034	-0.0031	-0.0029	-0.0027	-0.0025	-0.0023	-0.0022	-0.0021	-0.0020	-0.0019	-0.0018
5	-0.0037	-0.0033	-0.0030	-0.0028	-0.0025	-0.0023	-0.0021	-0.0020	-0.0018	-0.0017	-0.0016	-0.0015	-0.0014	-0.0013
6	-0.0028	-0.0025	-0.0023	-0.0021	-0.0019	-0.0017	-0.0016	-0.0014	-0.0013	-0.0012	-0.0011	-0.0010	-0.0009	-0.0008
7	-0.0019	-0.0017	-0.0015	-0.0014	-0.0012	-0.0011	-0.0009	-0.0008	-0.0007	-0.0006	-0.0005	-0.0004	-0.0003	-0.0002
8	-0.0008	-0.0007	-0.0007	-0.0005	-0.0004	-0.0003	-0.0002	-0.0001	-0.0000	0.0000	0.0001	0.0002	0.0003	0.0003
9	0.0003	0.0003	0.0003	0.0003	0.0004	0.0004	0.0005	0.0006	0.0007	0.0007	0.0008	0.0008	0.0009	0.0010
10	0.0016	0.0014	0.0013	0.0013	0.0013	0.0013	0.0013	0.0013	0.0014	0.0014	0.0015	0.0015	0.0016	0.0016
11	0.0029	0.0026	0.0024	0.0023	0.0022	0.0022	0.0021	0.0021	0.0022	0.0022	0.0022	0.0022	0.0023	0.0023
12	0.0043	0.0038	0.0035	0.0033	0.0032	0.0031	0.0030	0.0030	0.0030	0.0030	0.0030	0.0030	0.0030	0.0030
13	0.0058	0.0052	0.0047	0.0044	0.0042	0.0041	0.0040	0.0039	0.0038	0.0038	0.0038	0.0038	0.0038	0.0038
14	0.0075	0.0066	0.0060	0.0056	0.0053	0.0051	0.0050	0.0048	0.0048	0.0047	0.0047	0.0046	0.0046	0.0046
15	0.0092	0.0081	0.0074	0.0069	0.0065	0.0062	0.0060	0.0058	0.0057	0.0056	0.0056	0.0055	0.0055	0.0054
16	0.0109	0.0097	0.0088	0.0081	0.0077	0.0073	0.0070	0.0068	0.0067	0.0065	0.0064	0.0064	0.0063	0.0063
17	0.0129	0.0114	0.0103	0.0096	0.0090	0.0086	0.0082	0.0080	0.0078	0.0076	0.0075	0.0074	0.0073	0.0072
18	0.0149	0.0131	0.0119	0.0110	0.0103	0.0098	0.0094	0.0091	0.0088	0.0086	0.0085	0.0084	0.0082	0.0082
19	0.0169	0.0150	0.0136	0.0125	0.0117	0.0111	0.0107	0.0103	0.0100	0.0097	0.0095	0.0094	0.0093	0.0091
20	0.0191	0.0169	0.0153	0.0141	0.0132	0.0125	0.0120	0.0115	0.0112	0.0109	0.0107	0.0105	0.0103	0.0102
21	0.0213	0.0189	0.0171	0.0157	0.0147	0.0139	0.0133	0.0128	0.0124	0.0121	0.0118	0.0116	0.0114	0.0112
22	0.0237	0.0209	0.0189	0.0174	0.0163	0.0154	0.0147	0.0141	0.0137	0.0133	0.0130	0.0127	0.0125	0.0123
23	0.0262	0.0231	0.0209	0.0192	0.0179	0.0169	0.0161	0.0155	0.0150	0.0145	0.0142	0.0139	0.0137	0.0134

"The aeronautical and space activities of the United States shall be conducted so as to contribute . . . to the expansion of human knowledge of phenomena in the atmosphere and space. The Administration shall provide for the widest practicable and appropriate dissemination of information concerning its activities and the results thereof."

—NATIONAL AERONAUTICS AND SPACE ACT OF 1958

NASA SCIENTIFIC AND TECHNICAL PUBLICATIONS

TECHNICAL REPORTS: Scientific and technical information considered important, complete, and a lasting contribution to existing knowledge.

TECHNICAL NOTES: Information less broad in scope but nevertheless of importance as a contribution to existing knowledge.

TECHNICAL MEMORANDUMS: Information receiving limited distribution because of preliminary data, security classification, or other reasons.

CONTRACTOR REPORTS: Scientific and technical information generated under a NASA contract or grant and considered an important contribution to existing knowledge.

TECHNICAL TRANSLATIONS: Information published in a foreign language considered to merit NASA distribution in English.

SPECIAL PUBLICATIONS: Information derived from or of value to NASA activities. Publications include conference proceedings, monographs, data compilations, handbooks, sourcebooks, and special bibliographies.

TECHNOLOGY UTILIZATION PUBLICATIONS: Information on technology used by NASA that may be of particular interest in commercial and other non-aerospace applications. Publications include Tech Briefs, Technology Utilization Reports and Notes, and Technology Surveys.

Details on the availability of these publications may be obtained from:

SCIENTIFIC AND TECHNICAL INFORMATION DIVISION

NATIONAL AERONAUTICS AND SPACE ADMINISTRATION

Washington, D.C. 20546